FE-1749-7
Distribution Category UC-90c

MATERIALS RESEARCH FOR CLEAN UTILIZATION OF COAL

QUARTERLY PROGRESS REPORT
April 1976

Samuel J. Schneider
Project Manager

Institute for Materials Research
National Bureau of Standards
Washington, D. C. 20234

PREPARED FOR THE UNITED STATES
ENERGY RESEARCH AND DEVELOPMENT ADMINISTRATION

Under Contract No. 14-32-0001-1749

I. OBJECTIVE AND SCOPE OF WORK

Coal Gasification processes require the handling and containment of corrosive gases and liquids at high temperature and pressures, and also the handling of flowing coal particles in this environment. These severe environments cause materials failures which inhibit successful and long-time operation of the gasification systems. The project will entail investigations on the wear, corrosion, chemical degradation, fracture, and deformation processes which lead to the breakdown of metals and ceramics currently being utilized in pilot plants (and suffering failures). Studies will also be carried out on new candidate materials considered for improved performance. Special emphasis will be devoted to the development of test methods, especially short-time procedures, to evaluate the durability of materials in the gasification environments. These methods will focus on wear, impact erosion, stress corrosion, strength, deformation, slow crack growth and chemical degradation of refractories. Failure analysis of gasifier components, both metal and ceramic will be conducted as necessary. Failure reports from gasifiers will be compiled, abstracted and recommendations made to ERDA as to the appropriate action to be taken. All studies will be correlated with field inspections and failure analysis on in-service materials. Active consultation and proposal review services to ERDA and associated contractors will be provided.

II. SUMMARY OF PROGRESS TO DATE

The summary of progress is contained in the individual task progress and plans - Section III. See Performance Chart following.

III. DETAILED DESCRIPTION OF TECHNICAL PROGRESS

1. Durability and Reliability of Materials of Construction

A. Metals

a) Corrosion (G. M. Ugiansky and C. E. Johnson, 312.04)

Progress: Work has continued with the testing of 310 stainless steel specimens over a range of strain-rates in H_2O/H_2S gaseous mixtures at 1000°F, H_2S at room temperature and at 1000°F, and dry He at room temperature and 1000°F. We feel that the tests that we have completed with the constant strain-rate method with the gaseous system of known susceptibility to stress corrosion cracking (SCC) give us sufficient reason to believe that a measure of elongation versus strain-rate is a reasonable measure of susceptibility to SCC. However, a better general fracture criterion might also include a measure of reduction in area (some data for this is given in this report) or some combination of elongation and reduction in area.

Tests have been run at strain rates as low as $8.43 \cdot 10^{-7}\ S^{-1}$ which is near the lower limit of our machines as they are presently set up. Even at this strain-rate, the area of greatest susceptibility for 310 SS in H_2O/H_2S gaseous mixture at 1000°F has not been reached as seen in Fig. 1 and Fig. 2. That is, the minimum in the curves has not been reached.

Several specimens were tested in H_2S at room temperature (Fig. 1 and Fig. 2). No visible cracks were detected and the fractures were ductile. Only very slight corrosion was detected on the surface of the specimens. One notable test was the specimen tested at 1000°F in dry He inside a stainless steel (SS) furnace tube that had been used for tests run in H_2O/H_2S gaseous mixture at 1000°F. Evidently the SS tube has been attacked and some sulfide products were present on the walls of the tube. When the test was done at 1000°F with dry He, there was enough sulfur present to cause SCC and brittle fracture in the 310 SS specimen. It appears that a low concentration of sulfur will cause SCC at 1000°F at a low strain rate.

Fig. 3 shows surface scale and some small secondary cracks on the 310 SS specimen that was tested in dry He at 1000°F in the furnace tube that contained some sulfur containing corrosion products on the walls. The constant strain-rate for that test was $8.429 \cdot 10^{-7}\ S^{-1}$. Fig. 4 shows the secondary cracking in the same specimen as in Fig. 3 after the surface scale was removed.

Several 310 SS specimens were also tested in pure H_2S (that is, H_2S straight from the tank with no additives) atmospheres at 1000°F over a range of strain-rates. The susceptibility to SCC seems to be just as great in the pure H_2S atmosphere as it was for the H_2O/H_2S gaseous mixture. Figs. 5, 6, and 7 show stress-strain curves for the 310 SS specimens tested in pure H_2S at 1000°F at constant strain-rates of $7.80 \cdot 10^{-5}\ S^{-1}$, $3.95 \cdot 10^{-6}\ S^{-1}$, $1.06 \cdot 10^{-6}\ S^{-1}$, respectively.

Another 310 SS specimen was tested at the slow strain-rate of $8.429 \cdot 10^{-7}$ S^{-1} in dry He at 1000°F (Fig. 8). This compares with the specimen in Figs. 3 and 4 except that the 304 SS furnace tube was replaced with a new, clean one without any sulfide contamination. The He was passed through a liquid nitrogen cold trap before entering the furnace tube at a rate of approximately 1 cm^3/sec. Again the specimen showed a brittle fracture with secondary cracking. Some oxide or other corrosion product film was apparent on the surface of the specimen indicating that some of the impurities in the helium might be significant.

Elongations vs. strain-rate for the 310 SS specimens tested in pure H_2S atmosphere at 1000°F along with the specimen tested in dry He at 1000°F are shown in Fig. 9. Reduction in area vs. strain-rate for the same specimens are shown in Fig. 10. The data for the specimens tested in H_2S compare favorably with the data obtained when testing in H_2O/H_2S gaseous mixture.

The cause of the extreme sensitivity of 310 SS to SCC at 1000°F even in He (the purity of which is given in the table below) is our main concern at this time.

Purity and Permissible Impurities

Properties	Acceptable Limits
Helium	99.995 pct min.
Dew Point (Degrees F)	-90
Water (at 200 psig)	3.5 ppm max.
Hydrocarbon (condensed)	0
Hydrocarbon (as Methane)	1.0 ppm max.
Oxygen	1.5 ppm max.
Argon	1.0 ppm max.
Nitrogen	8.0 ppm max.
Neon	20.0 ppm max.
Hydrogen	.5 ppm max.
Carbon dioxide	.5 ppm max.
Carbon monoxide	.5 ppm max.
Other Gases	1.0 ppm max. each
Time allowable Impurities	50 ppm

There are several possible explanations for the oxide formation and the brittle fracture at the slow strain rates in the He. Even though the water and oxygen contents are low in the He gas, there may be enough to cause the formation of chromium oxide at some critical temperature. A titanium gettering furnace will be used to try to solve this problem.

As for the brittle fracture and cracking, it was thought that sensitization of the 310 SS may be occurring when testing at the slow strain-rates because of the longer time at temperature and that the sensitation would cause a decrease in ductility. Several specimens were allowed to soak at 1000°F for 72 hours

in dry He and also in H_2S under a no-load condition. The time was equivalent to the total time of exposure to 1000°F when a specimen was pulled at the slow strain-rate of $8.429 \cdot 10^{-7}$ S^{-1}. The specimens were then pulled at a faster strain-rate where a ductile fracture was known to occur under our normal non-soaking at temperature tests. If a brittle fracture occurred, then time at temperature was a factor in producing some phase of lower strength. Fig. 11 is a stress-strain curve of a 310 SS specimen soaked in dry He at 1000°F for 72 hours under no load. The specimen was cooled to room temperature and tested in dry He at a constant strain-rate of $7.1808 \cdot 10^{-6}$ S^{-1}. That specimen was quite ductile and compared with other test at room temperature. Fig. 12 is a stress-strain curve of a 310 SS specimen soaked in dry He at 1000°F for 72 hours under no load. The specimen was cooled to room temperature then tested in dry He at 1000°F at a constant strain-rate of $1.301 \cdot 10^{-4}$ S^{-1} in a new 304 SS furnace tube. A light film of oxide formed, but the fracture again was ductile. Fig. 13 is a stress-strain curve of a 310 SS specimen soaked in H_2S at 1000°F for 72 hours under no load. The specimen was cooled to room temperature then tested in dry He at 1000°F at a constant strain-rate of $1.301 \cdot 10^{-4}$ S^{-1}. The fracture was ductile and the curve compares closely to the one soaked in dry He and tested in dry He at 1000°F. It appears that if sensitization is occurring it alone is not causing the decrease in ductility when testing at the slow strain-rates.

If sensitization is involved in the cracking mechanism, it is not a sufficient reason for cracking. However, we do know that slow straining at temperature is a necessary condition for the cracking phenomenon. We believe that it is the impurities on the helium that are also a necessary condition for cracking to occur. Therefore, attempts are underway to find a truly "inert" atmosphere in which we can test specimens to form a data base to normalize to. As mentioned above, we are now doing everything possible to get ultra-high purity helium into the test cell.

The calibration of the last two furnace controllers has been completed. This now gives us full use of all four constant strain-rate testing machines.

A few problems arose in the electronics of the data gathering facility. These problems were recognized and corrected.

Plans: Continue to study the reason for the brittle fracture occurring when testing in dry He at 1000°F at slow strain-rates. Build cell and machine specimens for testing 4340 in aqueous sodium chloride solution using the constant strain-rate machines.

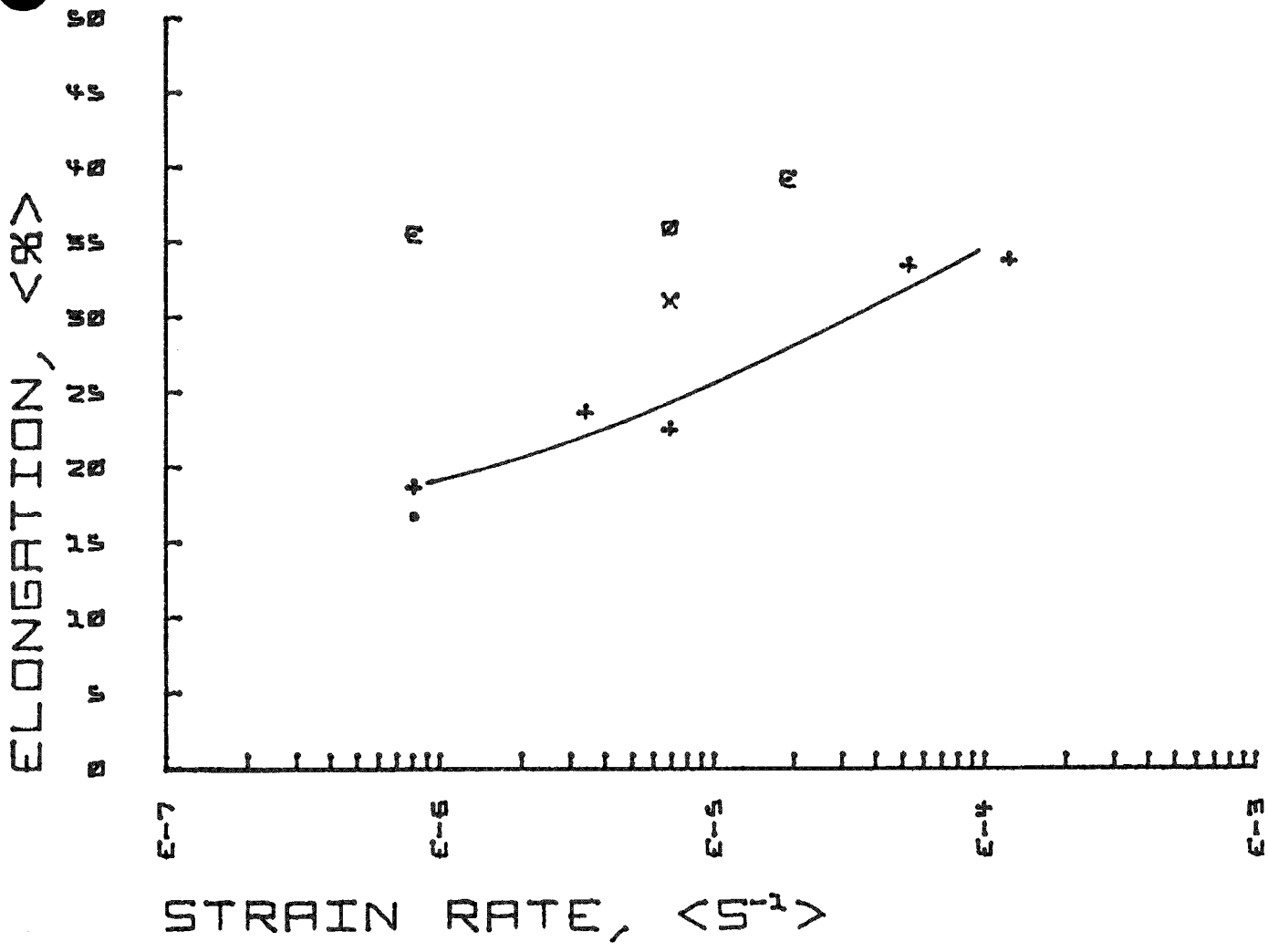

Fig. 1. Elongation vs. strain rate for 310 stainless steel in H_2O/H_2S gaseous mixture at 1000°F (+). The (O) point indicates a 310 SS specimen run at room temperature in dry He. The (X) point indicates a 310 SS specimen run at 1000°F in dry He. The (•) point indicates a 310 SS specimen run in dry He at 1000°F in a stainless steel furnace tube that had sulfide corrosion products on the walls from previous test runs. The (E) points indicate 310 SS specimens run in pure H_2S at room temperature. These elongation data were measured from the one inch gage length on the specimens.

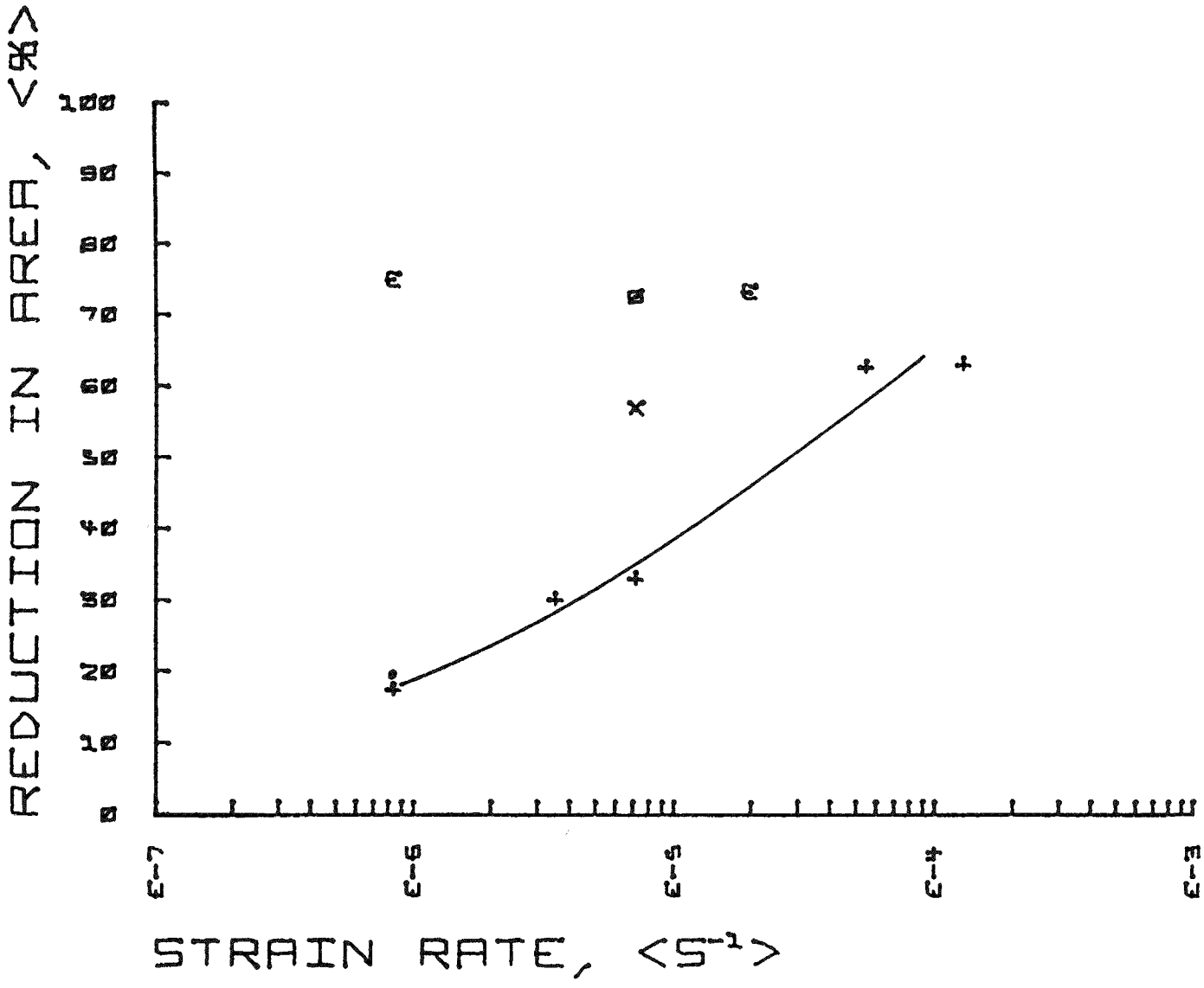

Fig. 2. Reduction in area vs. strain rate for 310 stainless steel in H_2O/H_2S gaseous mixture at 1000°F (+). The (O) point indicates a 310 SS specimen run at room temperature in dry He. The (X) point indicates a 310 SS specimen run at 1000°F in dry He. The (•) point indicates a 310 SS specimen run in dry He at 1000°F in a stainless steel furnace tube that had sulfide corrosion products on the walls from previous test runs. The (E) points indicate 310 SS specimens run in pure H_2S at room temperature.

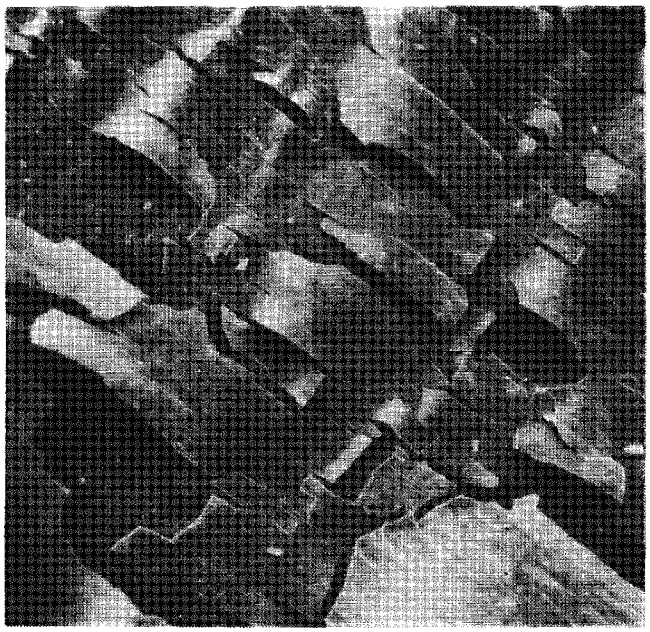

Fig. 3. Scanning electron micrograph showing surface scale on cold-drawn 310 SS tested in dry He at 1000°F in a 304 SS furnace tube whose interior wall was coated with sulfur corrosion products. Constant strain rate was $8.429 \cdot 10^{-7}$ S^{-1}. 130 X.

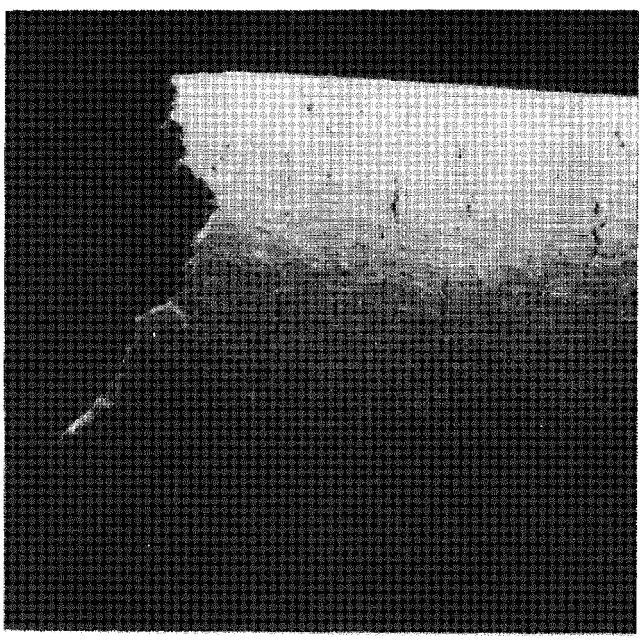

Fig. 4. Scanning electron micrograph showing secondary cracking after removal of surface scale on cold-drawn 310 SS tested in dry He at 1000°F in a 304 SS furnace tube whose interior wall was coated with sulfur corrosion products. Constant strain rate was $8.429 \cdot 10^{-7}$ S^{-1}. 20 X.

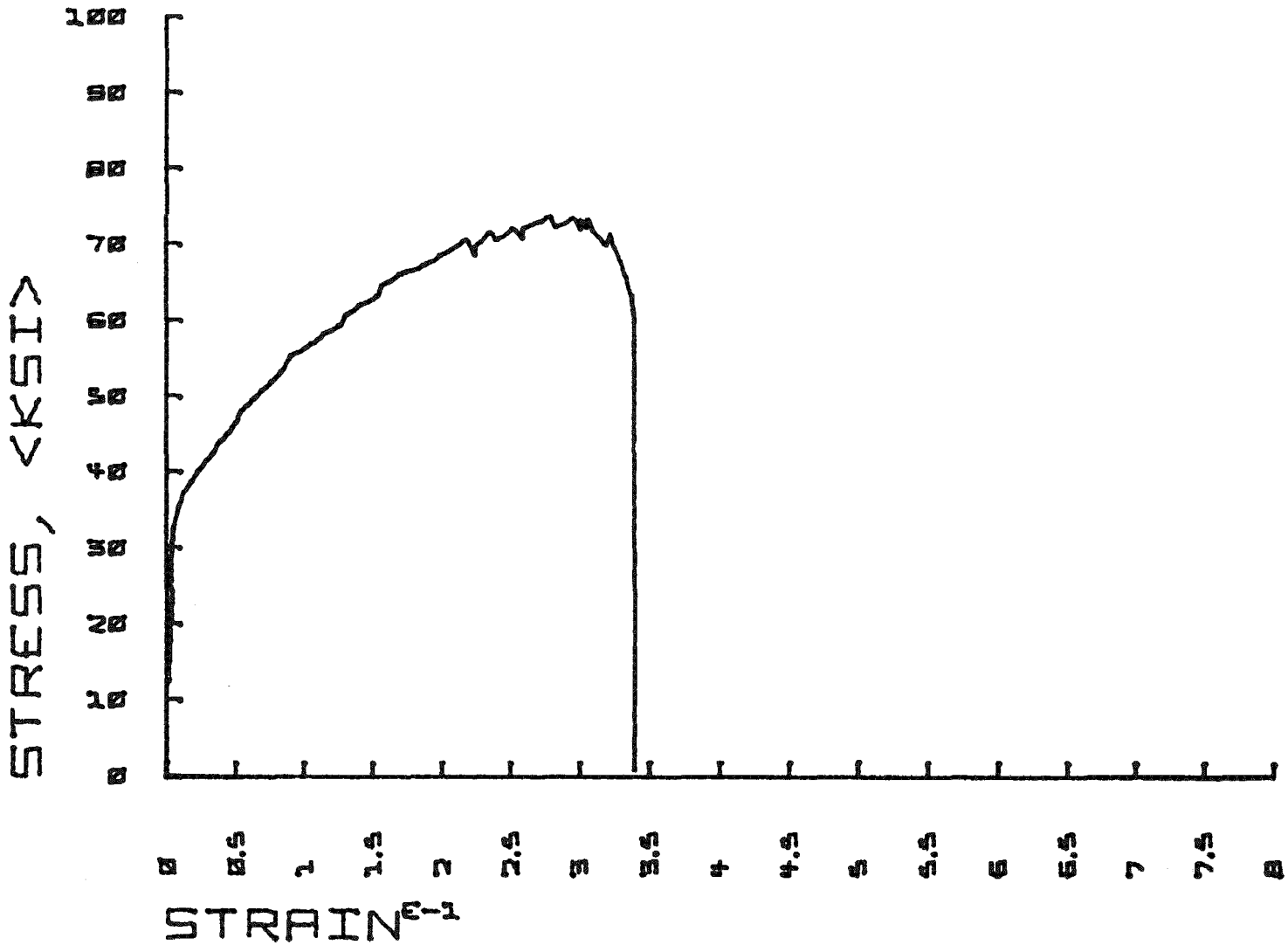

Fig. 5. Stress-strain curve for colled rolled 310 stainless steel in H_2S @ 1000°F at a constant strain rate of $7.80 \cdot 10^{-5}$ s^{-1}.

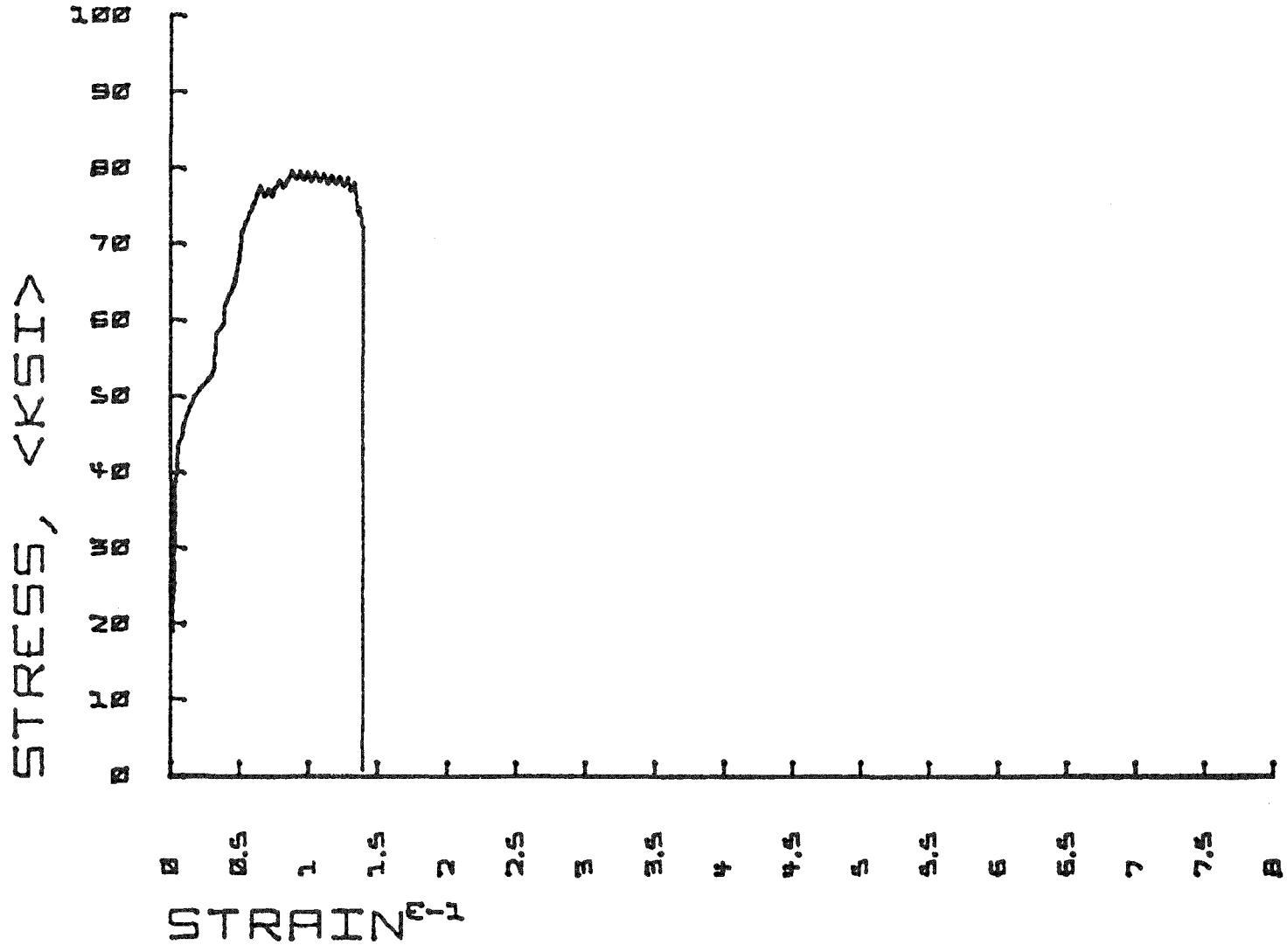

Fig. 6. Stress-strain curve for colled rolled 310 stainless steel in H_2S @ 1000°F at a constant strain rate of $3.946 \cdot 10^{-6}$ S^{-1}.

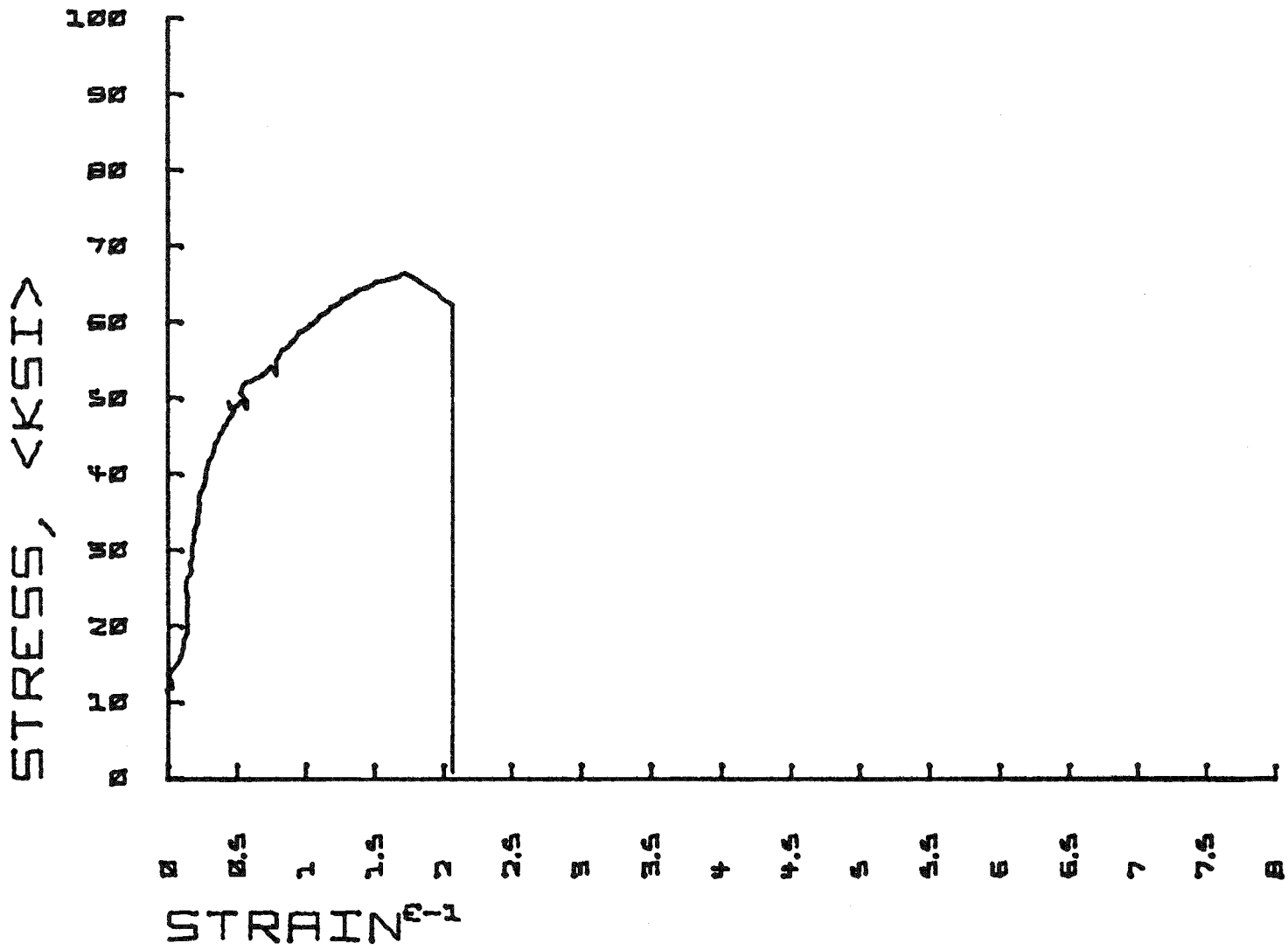

Fig. 7. Stress-strain curve for cold rolled 310 stainless steel in H_2S @ 1000°F at a constant strain rate of $1.059 \cdot 10^{-6}$ s^{-1}.

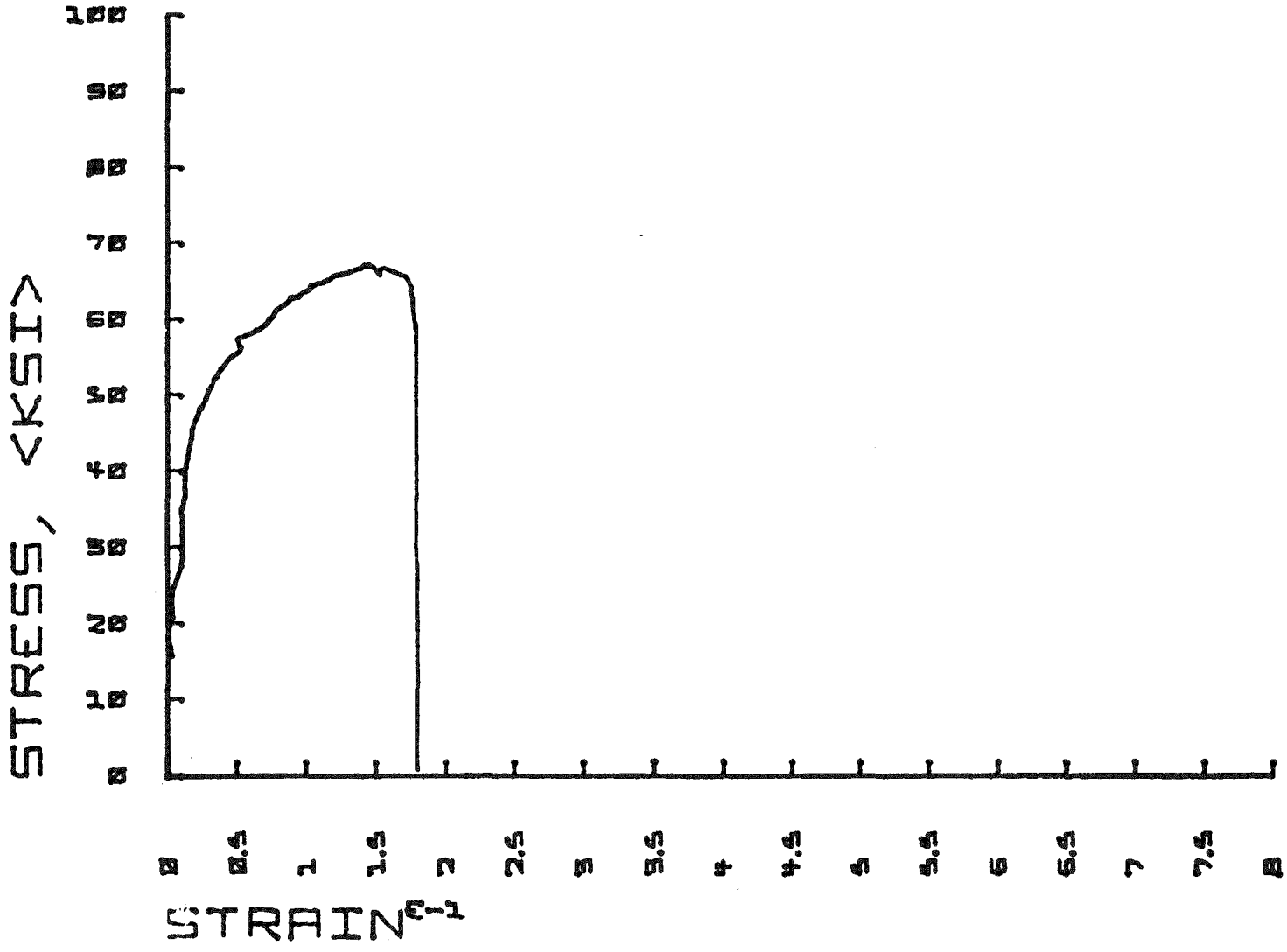

Fig. 8. Stress-strain curve for cold rolled 310 stainless steel in dry He @ 1000°F at a constant strain rate of $8.429 \cdot 10^{-7}$ S^{-1}. Test was made in a new clean 304 SS furnace tube.

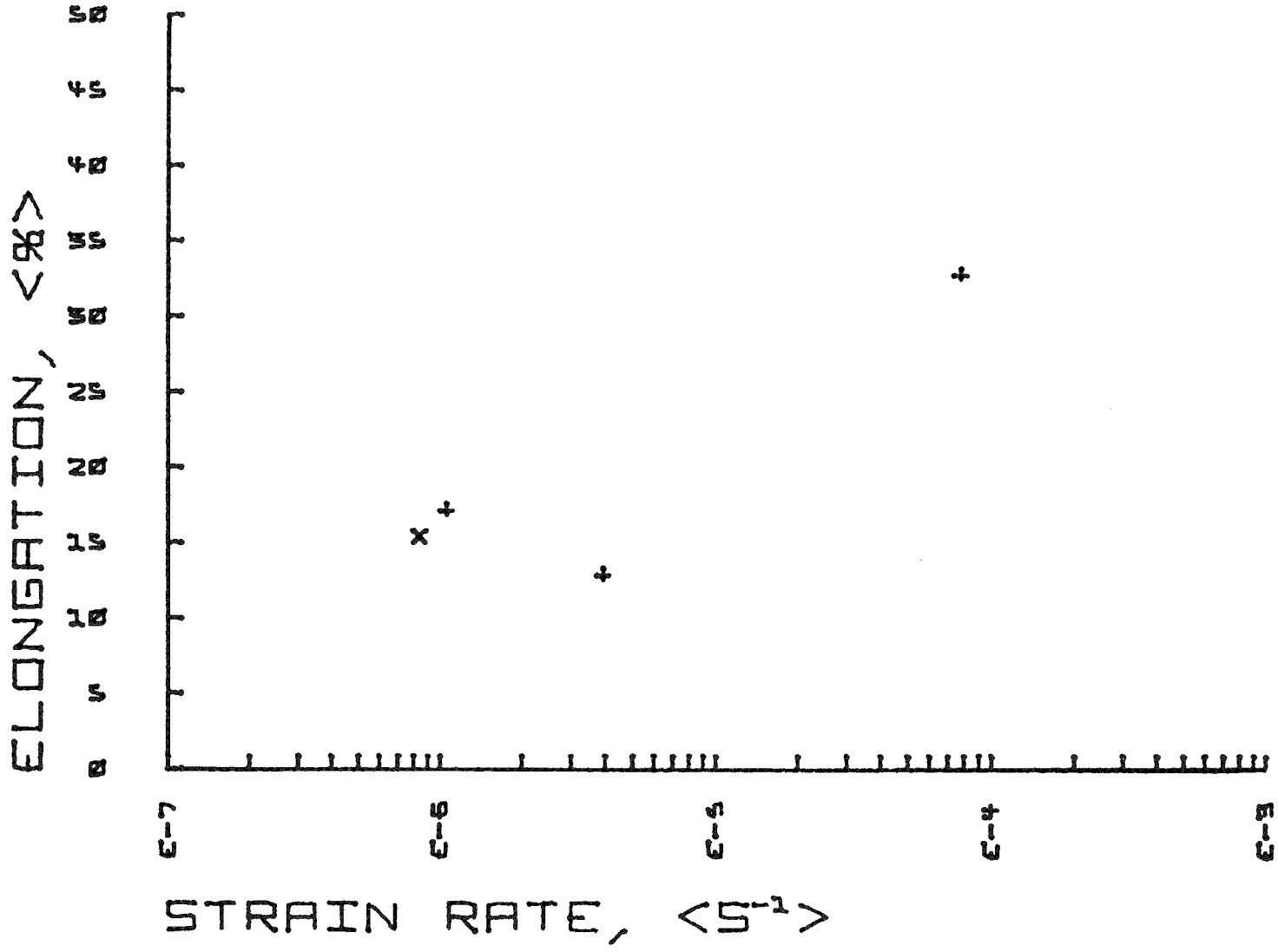

Fig. 9. Elongation vs. strain rate for 310 stainless steel in H_2S at 1000°F (+). The (X) point indicated a 310 SS specimen run at 1000°F in dry He in a new, clean 304 SS furnace tube. The elongation data were measured from the one inch gage length on the specimens.

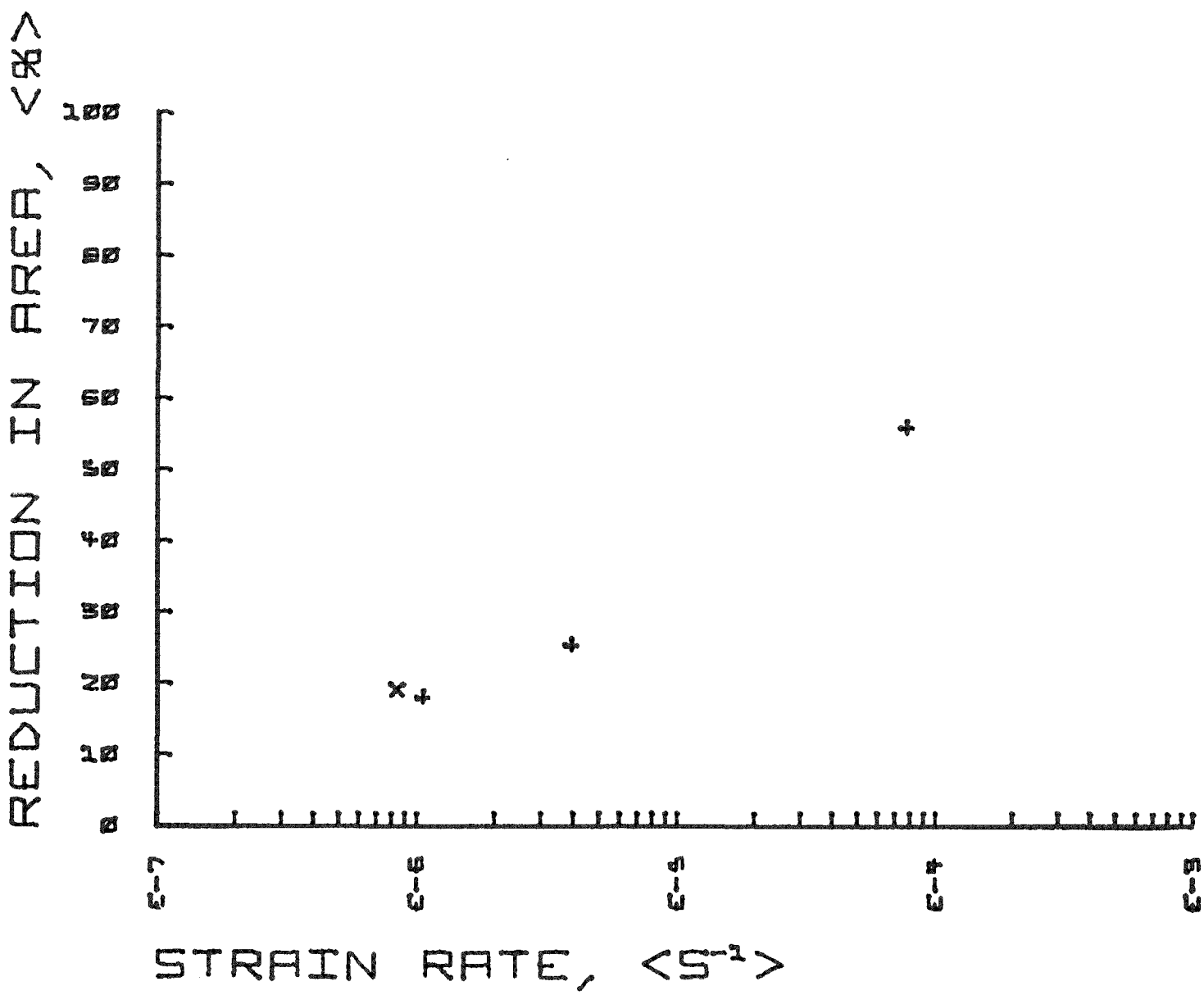

Fig. 10. Reduction in area vs. strain rate for 310 stainless steel in H_2S at 1000°F (+). The (X) point indicates a 310 SS specimen run at 1000°F in dry He in a new, clean 304 SS furnace tube.

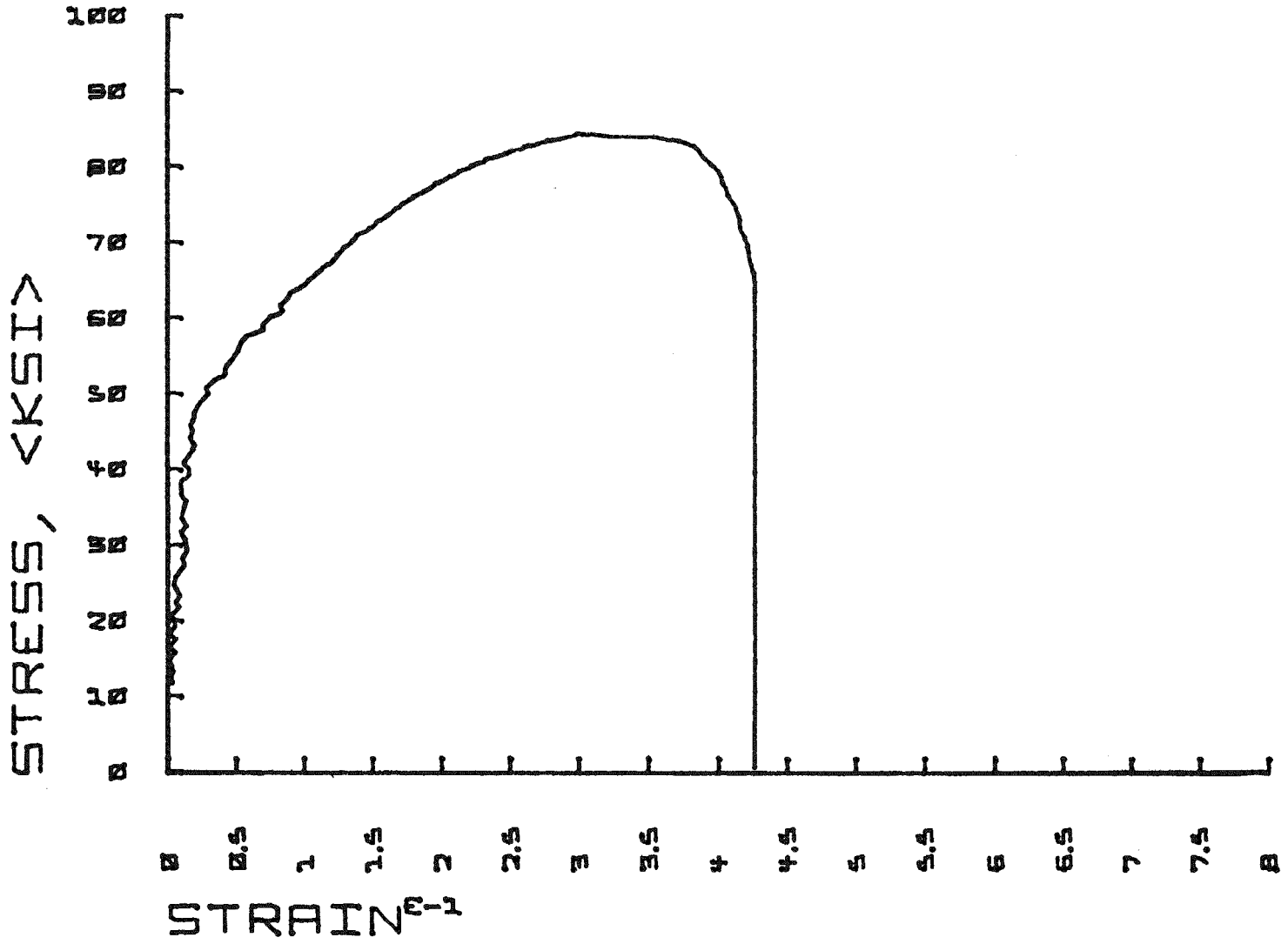

Fig. 11. Stress-strain curve for cold rolled 310 stainless steel in dry He at room temperature at a constant strain rate of $7.1808 \cdot 10^{-6}$ s^{-1} after being held for 72 hours at 1000°F in dry He under a no-load condition.

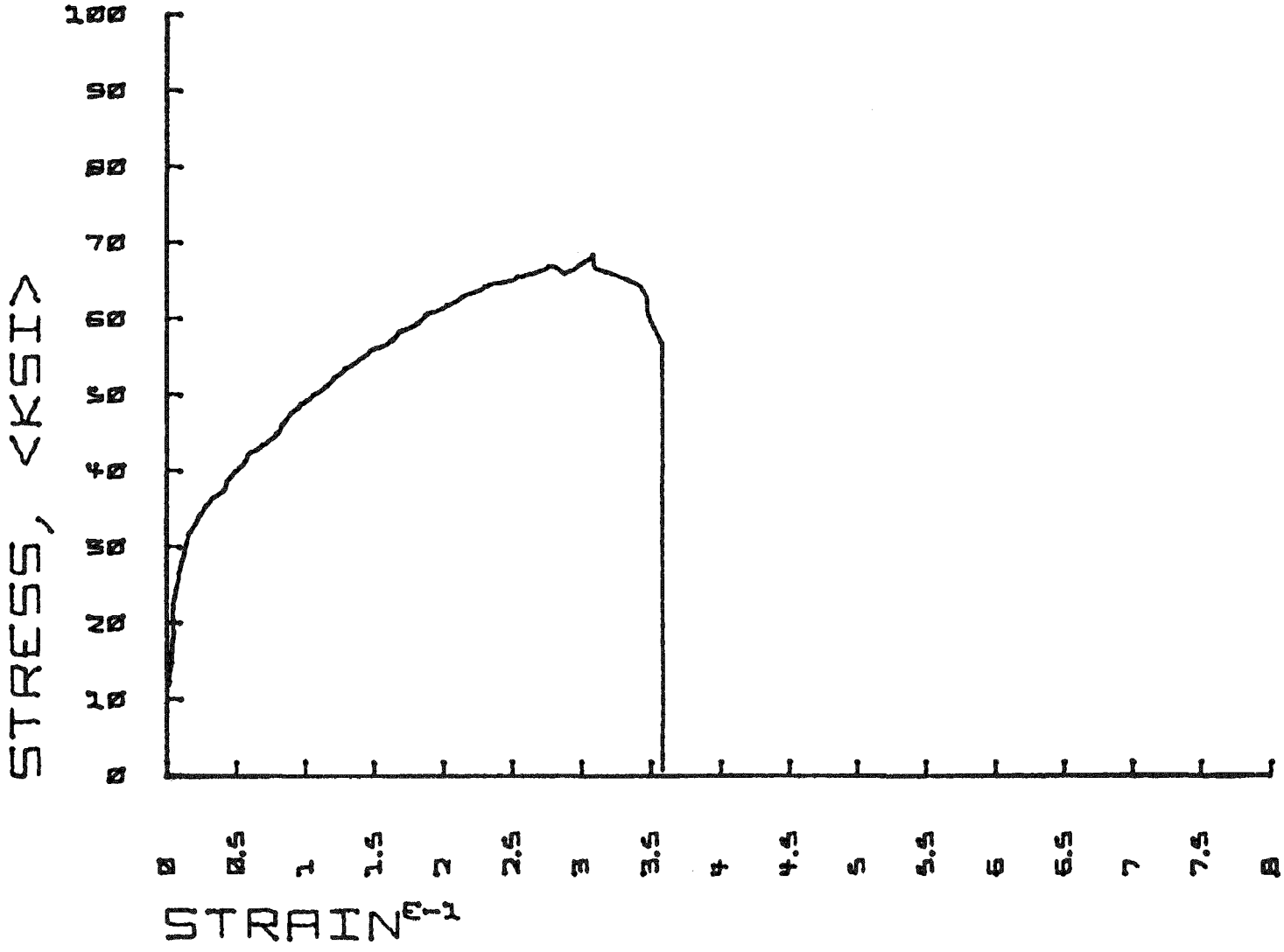

Fig. 12. Stress-strain curve for cold rolled 310 stainless steel in dry He at 1000°F at a constant strain rate of $1.301 \cdot 10^{-4}$ s^{-1} after being held for 72 hours at 1000°F in dry He under a no-load condition. Specimen was allowed to cool to room temperature before test was run.

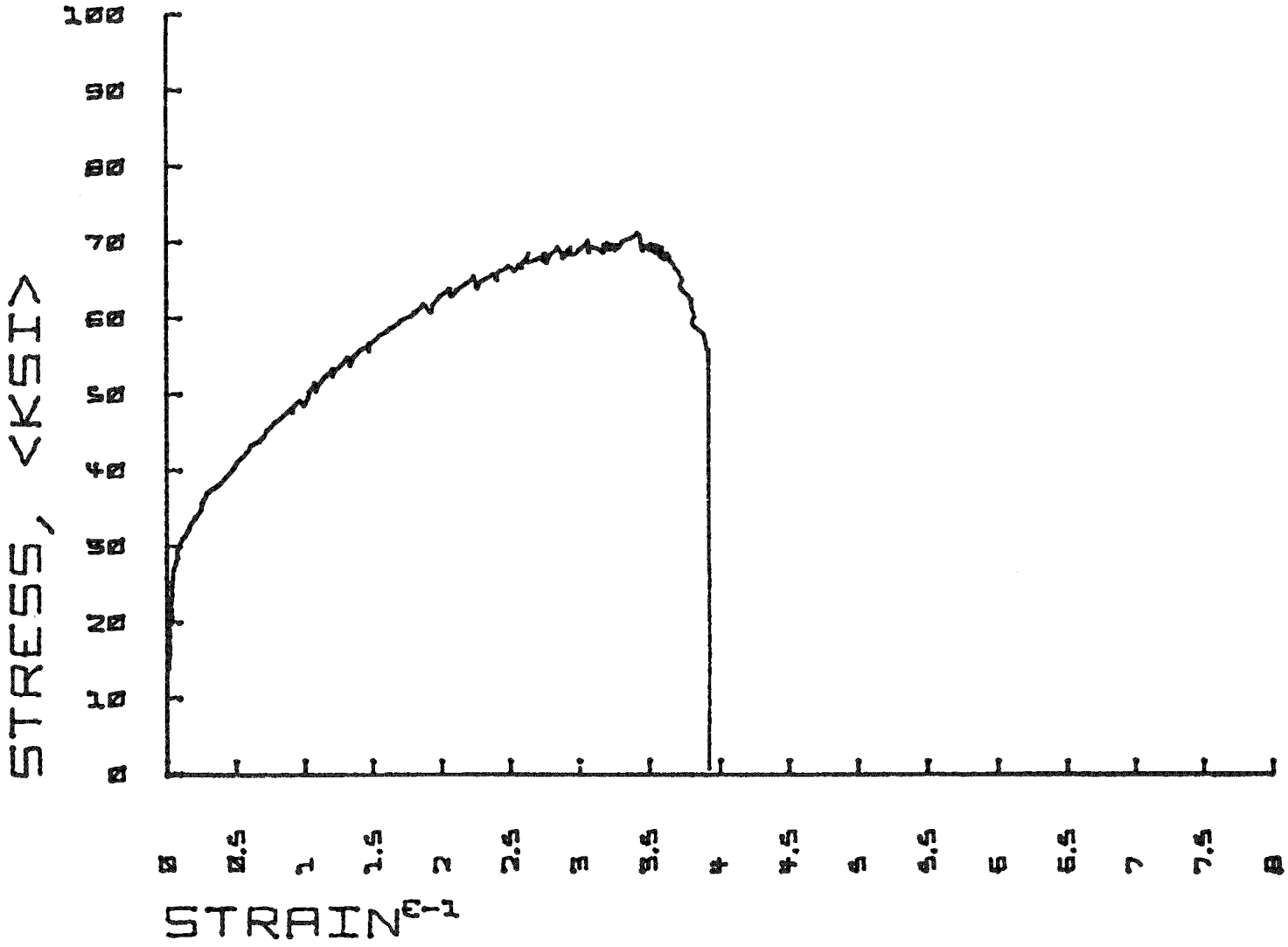

Fig. 13. Stress-strain curve for cold rolled 310 stainless steel in dry He at 1000°F at a constant strain rate of $1.301 \cdot 10^{-4}$ S^{-1} after being held for 72 hours at 1000°F in H_2S under a no-load condition. Specimen was allowed to cool to room temperature before test was run.

b) Erosive Wear (A. W. Ruff, L. K. Ives, J. P. Young, 312.03)

Progress: The eight foot length of metal tubing used to preheat the propellant gas and abrasive in the Roberts Abrader perforated at two of the 180° bends (at about 45° angle) after 20 hours of use. Abrasives passed through the tubing varied from 5 μm Al_2O_3 to 150 μm SiC and included substantial amounts of pumice and silica. Pertinent data are shown below:

Tubing material -- 304 stainless steel, 1/16 inch ID, 0.035 inch wall.

Pressure -- 10-70 psig, mostly 40 psig operation.

Temperature -- 25°C (5.3 hours at 300-500°C).

Abrasive velocity -- Estimated 30 m/s average.

Propellant gas -- CO_2 principally.

Calculated rate of wear -- 1.8 mil/hr.

The wear rate of 304 stainless steel test specimens has been about 17 mil/hr at v = 50 m/s, reasonably consistent with the above result considering the effect of the increased velocity.

Pressure measurements made using a pressure transducer located just before the nozzle of the abrader unit showed that the pressure of the gas-abrasive stream was slightly reduced in proportion to the amount of abrasive entrained into the stream. The rate of abrasive flow is presently controlled by an electric vibrator attached to the abrasive storage chamber. By using a pressure transducer with an output of about 0-1 volt to sense the propellant gas pressure at the nozzle, the resultant electrical signal could be used to control the current flow to the vibrator on the abrasive chamber. An electronic device is being built which will amplify the signal from the transducer to control the current supply through an SCR to the vibrator. The device will also contain a 12 vDC power supply to operate the pressure transducer. The equipment should automatically maintain the desired pressure level and thus the abrasive flow rate to the nozzle. Presently abrasive flow constancy is attempted manually through control of the level in the abrasive chamber.

It has recently been observed that variations in propellant gas temperature also cause pressure changes at the nozzle when specimens are being tested at elevated temperatures and the gas and abrasive are being heated. Presumably this effect is related to the gas density changes as well as to abrasive loading fluctuations. It is felt that these pressure changes can be controlled by placing a thermocouple near the nozzle which would provide a signal suitable for pressure control. With these two additions to the Roberts abrader, more effective control of the abrasive velocity and flux reaching the specimen will be realized. This should further increase the reliability of the data obtained. We expect that the final configuration of the erosion tester will allow the use of a substantial range of particle sizes, particle velocities and particle fluxes for

erosion testing of metals, coatings and ceramics in various atmospheres at temperatures up to 1000°C. It should be possible to conduct tests quickly and conveniently using relatively unskilled personnel.

Studies are underway on the effect of using propellant gases other than CO_2 on the erosion rate of 304 stainless steel at elevated temperatures. Preliminary checks indicated oxide formation at 1000°C was about the same for O_2 and CO_2 while less oxide was formed on the area of the specimen impinged by the jet of N_2. A comparison of the results of the four propellant gases is shown below (0.5 mm nozzle, 45°, 1 cm, 50 μm Al_2O_3, 40 psig, 2 min.):

Propellant Gas	Relative Wt. Loss (mg/g abr.)			Relative Penetration (μm/g abr.)		
	250°C	500°C	1000°C	250°C	500°C	1000°C
CO_2	-----	0.33	0.93	-----	7.8	20.6
CO (20% in N_2)	0.09	0.22	0.44	5.6	7.5	12.8
O_2	0.23	0.33	0.71	6.0	10.5	14.6
N_2	-----	0.36	0.64	-----	11.5	17.0

The comparative wear in this test indicates there is some protective effect at elevated temperatures of the continuous formation of oxide at the abraded surface when O_2 is used as the propellant gas. The apparent lower erosion rate obtained using CO as a propellant gas may be the result both of a reduced oxidation rate and an increased amount of sintering of the abrasive on the specimen surface in this reducing atmosphere. The appearance of the eroded surface of a specimen tested in a 20% CO atmosphere is shown in Fig. 1 along with micrographs showing examples of all the specimens tested at 1000°C.

A new alloy, Haynes 8077, containing 16% Cr, 4% Al plus Ni and Y_2O_3 was tested in the jet abrader at 25°C. 50 μm Al_2O_3 was used with the nozzle at 45° and 1 cm from the specimen. Test duration was the standard two minutes. The results were compared with those of several alloys previously tested using the same conditions as shown below:

Result	Alloy								
	304	310	316	250MS	671	446	601	800	8077
Mean wt. loss (mg)	4.9	0.9	1.0	1.3	1.1	0.5	3.1	3.3	2.4
Mean penetra. (μm)	268	89	90	91	91	59	203	203	80
$\frac{\text{Wt. loss}}{\text{Wt. abr.}}$ (mg/g)	0.47	0.09	0.10	0.13	0.11	0.05	0.30	0.32	0.16
$\frac{\text{Penetration}}{\text{Wt. abr.}}$ (μm/g)	25.8	8.6	8.7	8.8	8.8	5.7	19.5	19.5	5.3

The relative weight loss was greater than five of the other alloys but this initial test indicates somewhat less relative penetration at 25°C.

Further tests were carried out on 310 stainless steel specimens in the flame-erosion apparatus. Particle velocity (10-50 m/sec.) and gas composition were varied in these tests, while other parameters such as angle of attack (90°), particle type (SiC), particle size (100 mesh) and test duration (≈1 hr.) were held constant. All elevated temperature tests were carried out at about 975°C while for comparison purposes some tests were run at room temperature. The general thrust of our activities this quarter was to obtain a relatively complete set of data within the fairly restricted range of operating conditions indicated above. Particular attention was placed on characterizing those conditions. Gas samples were taken at the specimen location and submitted to the NBS Analytical Chemistry Division for analysis by mass spectrometry. Before discussing these results, however, it is important to describe an unexpected problem that arose in connection with the SiC abrasive material that has been employed in most of our tests.

We reported previously (October-December 1975 Quarterly Report) in describing tests at a velocity of 10 m/s under highly oxidizing conditions that significant amounts of SiC abrasive material appeared to adhere or sinter to the eroded surface. Often large clusters of particles were formed. A photograph of this phenomenon is shown in Fig. 2. It was also reported (January monthly) that sintering did not occur in similar tests under what were termed reducing conditions. It is now believed, on the basis of further tests under the oxidizing conditions in which little or no sintering occurred, that the effect was associated with the particular SiC abrasive material employed. Having exhausted a batch of SiC grit that had been used since the beginning of our program, a new supply obtained from the same company but at a later date was put into use. With this material very little sintering was observed regardless of gas composition or erosion rate. An equally significant and probably related effect observed with the new abrasive material was the substantly higher erosion rate at low velocities. Data obtained with both the new and old batches of SiC abrasive material are shown in Fig. 3. The two sets of data appear to converge at high velocities. The differences between the two lots of SiC are under investigation and will be reported later.

By changing the relative flow rate of oxygen, air, and propane, a range of different combustion gas environments can be obtained in the flame erosion apparatus at the sample location. However, both particle velocity and sample temperature also depend on the input gas flow. Particle velocity is determined mainly by the air flow while temperature is determined by all three components -- oxygen, air, and propane. Thus, control of the gas composition is restricted by the requirement that a chosen particle velocity and specimen temperature be maintained. In practice there is little difficulty in obtaining oxiding conditions at approximately 1000°C with particle velocities in the range 10-50 m/s. This is probably true for other achievable velocities and temperatures as well. Some gas compositions obtained at different velocities are shown below. Water vapor was not included in these analyses.

Particle Velocity	Gas Composition (%)					
	CO_2	CO	H_2	O_2	HC	N_2 + Ar
10 m/s	17.6	0	0	6.5	0	75.9
20	9.4	0	0	13.9	0	76.7
30	11.0	0	0	11.8	0	77.2

These conditions were produced by supplying excess oxygen and enough propane to obtain a temperature of ≈1000°C. The so-called reducing conditions are less easily achieved and maintained, particularly with the large excess of propane that is required to produce high CO/CO_2 ratios. Some results are shown below.

Particle Velocity (m/s)	Gas Composition (%)					
	CO_2	CO	H_2	O_2	HC	N_2 + Ar
10	11.0	11.2	6.3	Trace	Trace	71.4
20	6.4	23.4	15.8	0.2	1.2	53.0
30	6.0	13.9	9.7	1.7	5.6	63.1

Although relatively high concentrations of CO and H_2 were produced, small amounts of O_2 were also detected. This was probably a result of incomplete mixing and combustion in the gas stream at the sample location. Despite the fact that these conditions are judged to be oxidizing with respect to the 310 stainless steel alloy, the amount of oxide formed appeared to be notably less than at the strongly oxidizing condition described earlier. Spontaneous spallation of oxide scale from the eroded surface when the samples were cooled to room temperature after testing at less than about 25 m/s did not occur under the above conditions. Spalling was observed at low velocities regardless of the SiC abrasive material used when strongly oxiding conditions prevailed at the sample. The rate of erosion, however, does not appear to be significantly influenced by the different gas compositions employed in our tests. This is illustrated in Fig. 3 where the points denoted as strongly and weakly oxidizing do not indicate measurably different erosion rates at a given velocity.

It has been noted in previous reports that an induction period occurred at low velocities and low erosive rates prior to reaching steady state conditions. Some results of repeated tests are shown in Fig. 4. Each test lasted 1 hour and as many as 8 tests were carried out on a single sample. At 10 m/s, it is clear that up to 2 hours were required to reach an approximate steady state. Data plotted in Fig. 3 correspond to steady state conditions. Of course, there is no assurance that steady state has actually been reached. In particular, long-term oxidation effects may result in further changes in erosion rate after sufficient testing time has been accumulated.

A few room temperature tests have been carried out for comparison with elevated temperature results. The data are plotted in Fig. 3. The erosion rate at room temperature is approximately a factor of 10 less when compared with results obtained at 975°C with the second batch of SiC abrasive material. This difference is smaller with respect to the first batch of SiC at 975°C. On the basis of these few tests at room temperature, the erosion rate varies approximately as the velocity raised to the 2.3 power. This can be compared with velocity exponents of about 2.5 and 2.1 obtained for the first and second batches of SiC abrasive at 975°C, respectively. These data are subject to change, however, as more data is accumulated and the various parameters are better characterized.

With the cooperation of A. J. Liberatore of the Morgantown Energy Research Center, specimens have been installed in the MERC experimental gasifier system. Preparation of specimens, construction of mounting jigs, and installation of the completed assemblies were accomplished during this quarter. The specimens have been installed at three locations in the 25 inch diameter product gas output line leading from the top of the gasifier. Five different alloys will be exposed: 304, 446, 310, 800, and 671. A brief description of each location and the corresponding sample fixture follows:

Location 1. At the gas sampling port between the gasifier and the 1st pressure letdown orifice. The sample holder has been clamped in the 2 inch gas sampling pipe. The samples themselves are positioned directly in the product gas flow from the gasifier. The holder consists of two identical panels each containing eight 3/4 inch x 3/4 inch x 1/4 inch thick specimens. Five metal specimens and three ceramic specimens have been included. The angle of attack is 90° for one panel and 20° for the other.

Location 2. Just down stream of the first pressure letdown orifice. A single 1.5 cm diameter rod of 310 stainless steel is positioned for exposure to the high velocity jet of gases and particulate matter issuing from the pressure letdown orifice. On delivery of the specimen it was learned that the orifice had been temporarily removed so that the specimen will not be exposed to the high velocities anticipated.

Location 3. Down stream of the first pressure letdown orifice. The location is in a straight section of pipe at a considerable distance from bends and obstructions so that a relatively uniform flow of gas is expected. The holder consists of three panels similar to those at Location 1. The panels are oriented to obtain a different angle of attack at each panel, namely 20°, 45°, and 70°.

A test run of approximately one week duration is scheduled to commence and be completed this month (March). Upon completion of the run, the samples, will be removed for inspection. If little visible change has occurred, the samples will be reinstalled for further exposure. Evidence of significant changes will warrant removal of the samples to the laboratory for analysis.

Plans: Tests will continue using different gas atmospheres in the Roberts erosion apparatus. The automatic flux controller will be completed. Characterization of the SiC abrasives will be conducted. Design and construction of the high pressure erosion test unit will continue.

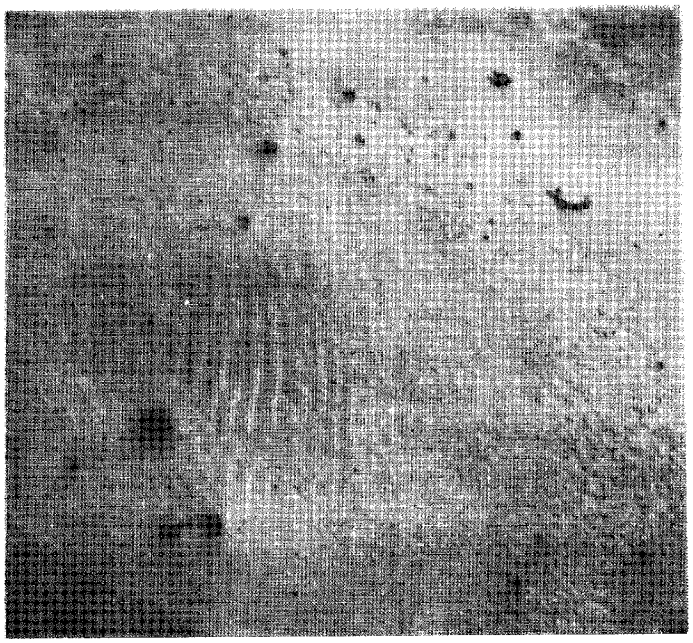

Fig. 1a Erosion crater, 304 stainless steel, 1000°C, CO_2, M = 16.

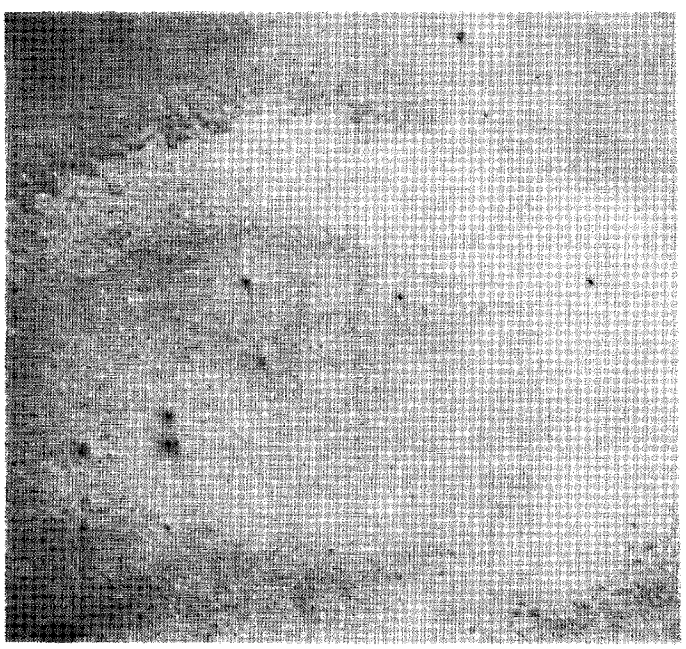

Fig. 1b Erosion crater, 304 stainless steel, 1000°C, CO, M = 16.

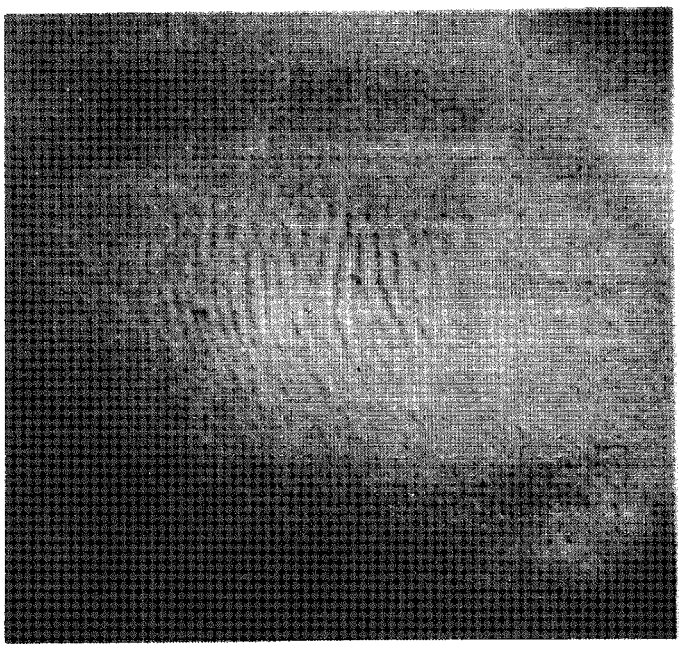

Fig. 1c Erosion crater, 304 stainless steel, 1000°C, O_2, M = 16

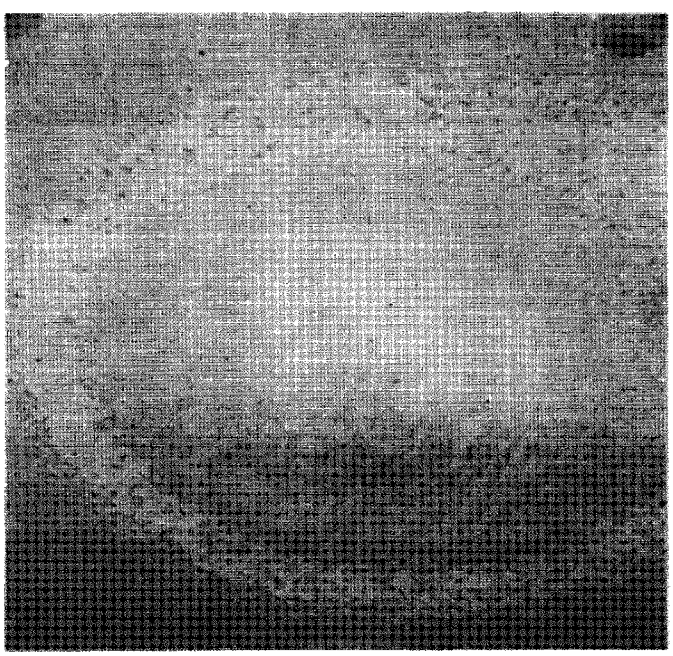

Fig. 1d Erosion crater, 304 stainless steel, 1000°C, N_2, M = 16.

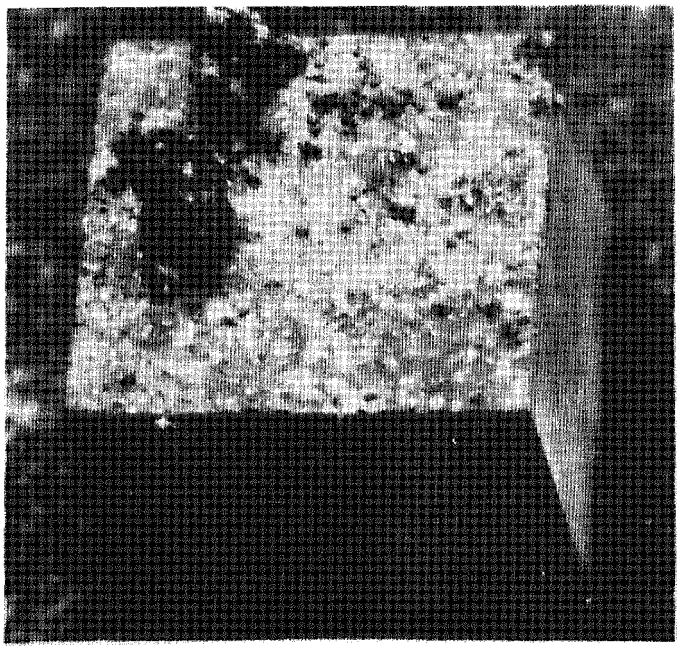

Fig. 2 Photograph of 310 ss specimen after testing with first batch of SiC abrasive material under strongly oxidizing conditions at 10 m/s particle velocity.

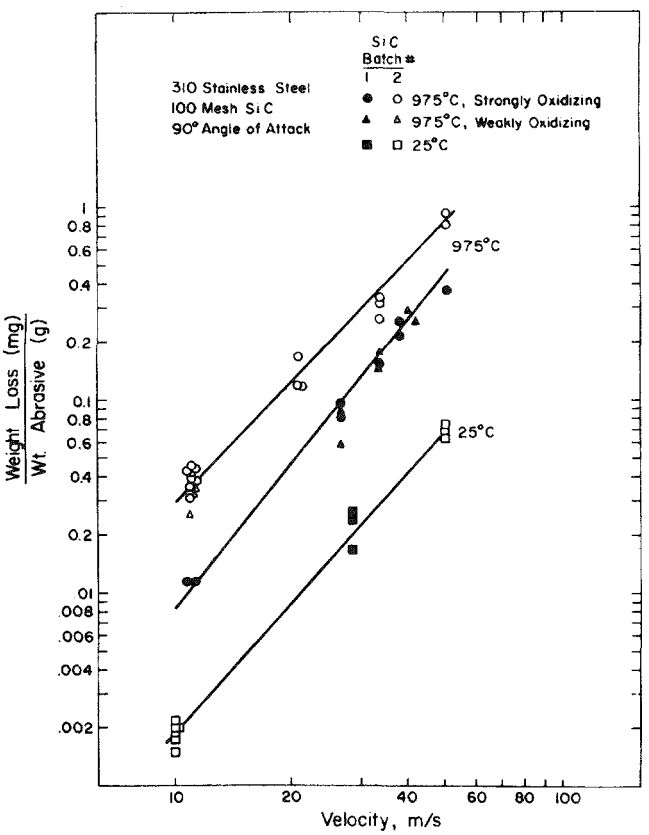

Fig. 3 Erosion results on 310 stainless steel.

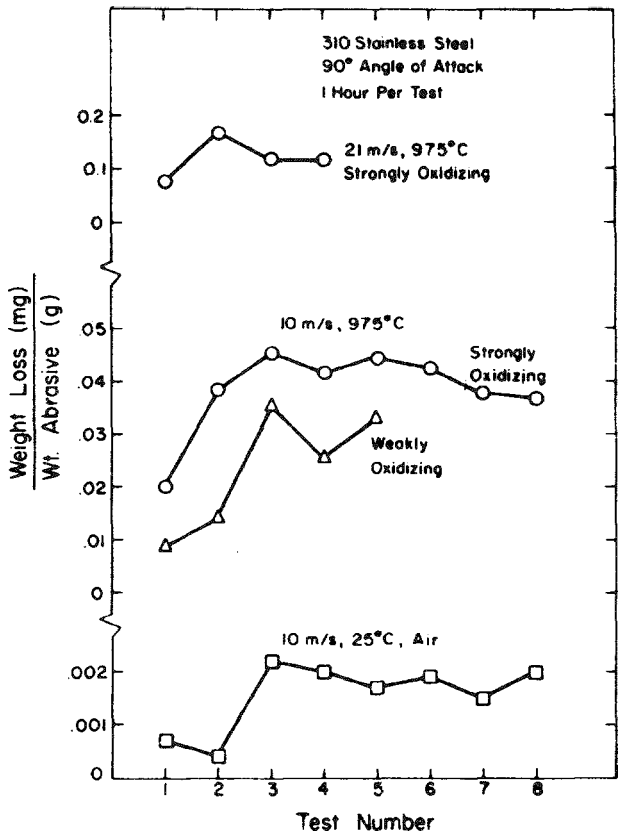

Fig. 4 Results of tests of one hour duration on 310 stainless steel. Each curve represents a different specimen.

B. Ceramics

a) Deformation and Fracture (E. R. Fuller, Jr., C. R. Robbins, and J. M. Bukowski, 313.05)

Progress: The main effort of the past quarter has been the procurement of elevated-temperature and -pressure equipment which can be used to expose ceramic refractory materials to various components of coal gasification systems, and the procurement of materials from which generic castable mixtures can be prepared for these studies. Several additional investigations have been undertaken. In one, effects of hydrothermal treatment on the flexural strength of two candidate commercial refractories have been examined. In another, the mineral phases have been determined for a piece of refractory lining from an operating coal gasifier. The results of this latter study are potentially very interesting depending on the initial status of the refractory. These efforts of the past quarter are detailed below.

Specifications for the procurement of a high-temperature, high pressure hydrothermal research unit have been released for bids by the Department of Commerce. The expanded capabilities of the two vessel systems will include operation at temperatures from room temperature to 960°C (1760°F), at pressures from atmospheric to 20 MPa (~ 2,900 psi), and in the presence of environments of H_2O, CO, CO_2, H_2, N_2, CH_4. and H_2S in various mixtures. Bid opening was in mid-March and the projected delivery date is May or June 1976.

In the interim, a hydrothermal vessel with a temperature capability of 600°C and a pressure limit of 35 MPa (~ 5,100 psi) has been made operative. The vessel pressure can be accurately measured, but cannot be precisely varied independent of temperature. Two pressure gauges allow operation at pressures from atmospheric to 3 MPa (~ 440 psi) and from atmospheric to 10 MPa (~ 1,450 psi). A temperature controlling unit has been installed on the vessel enabling the temperature to be accurately controlled and measured to within 5°C. However, the "cool down" period for the system is extremely long. Means to accelerate this "cool down" period are presently being examined. Brass molds are being constructed so that 12.5 x 25.0 x 120.0 mm refractory specimens can be cast for these studies. These specimens represent a "scale-up" in size by a factor of 2.5 over specimens which are being tested at present and will permit more quantitative flexural strength data to be obtained for ceramic systems containing aggregates of a larger particle size.

Various materials have been ordered so that generic castable mixtures can be prepared for these studies. To date, high-purity calcium-aluminate cements (CA-25 and SECAR 250) and refractory aggregates (tabular alumina, and calcined alumina) needed to produce these generic refractory compositions have been delivered. Delivery of refractory aggregates of calcined bauxite and calcined kaolin is expected as well as a set of screens with which to grade the various aggregates according to particle size.

Experiments performed in previous quarters indicated that the strength of calcium-aluminate-bonded castable refractory with calcined flint clay aggregate (55% alumina, 35% silica, 5% lime) seemed to be unaffected by high-pressure, high-temperature steam treatment. This property was investigated further this quarter. The hydrothermal treatment consists of sealing rectangular bend specimens and approximately 3 ml. of water in a pressure chamber and raising the temperature, thereby creating high-pressure steam. The specific volume of steam was approximately 4.5 ml/g. The temperature of hydrothermal treatment was varied from 110°C (230°F) to 510°C (950°F) with tests at: 110°C, 210°C, 375°C, 410°C, 510°C. The duration of each test condition was 20 hours. After exposure, the specimens were broken in four-point flexure at room temperature. In conjunction with task 1.B.b on Ceramic Erosion, specimens of this refractory and a high-purity, calcium-aluminate castable were treated hydrothermally in a similar manner for subsequent erosion studies at room temperature. X-ray diffraction patterns were taken on a specimen subjected to each hydrothermal condition to aid in the identification of the crystalline phases formed.

The room temperature bend strength after hydrothermal treatment is plotted in Figure 1 as a function of hydrothermal treatment temperature. Batch 1 are the results of previous experiments and batch 2 are the results of the present quarter. Each point represents the mean of the logarithm of the bend strength. The error bars represent the standard deviation of this quantity. Control specimens represent the strength before any hydrothermal treatment.

As indicated by Figure 1, there is no significant change in strength after exposure to hydrothermal treatment for the entire range of test temperatures. The difference in the flexural strength between batch 1 and batch 2 at the lower hydrothermal temperatures is probably a reflection of the mixing conditions. Batch 1 was mixed by hand; whereas batch 2 was prepared with a commercial mixer enabling a lesser amount of casting water to be used. This reduction in casting water probably results in a decreased porosity and hence, an increase in flexure strength. Interestingly, this difference is not as great for the higher hydrothermal temperatures, indicating possibly a change in porosity with hydrothermal treatment. Although an analysis of crystalline phases by means of an x-ray diffraction patterns is still in progress, preliminary results are given in Table 1.

Table 1. Preliminary analysis of predominant phases, as determined by x-ray diffraction patterns, of a calcium-aluminate-bonded castable with calcined flint clay aggregate as a function of hydrothermal treatment temperature. Phases listed in apparent order of abundance with exception of unidentified phase(s).

Temperature	Phases*
Room Temperature	cristobalite, mullite (A_3S_2), α-alumina, CA_2, CA, amorphous material, unidentified phase(s).
110°C 230°F	cristobalite, mullite, α-alumina, gibbsite (AH_3), C_3AH_6, unidentified phase(s).
310°C 590°F	mullite, cristobalite, α-alumina, boehmite (AH), $C_4A_3H_3$, C_3AH_6, unidentified phase(s).
410°C 770°F 510°C 950°F	mullite, cristobalite, α-alumina, unidentified phase(s).

* Cement chemistry notation used is:

C = CaO; A = $A\ell_2O_3$; S = SiO_2; and H = H_2O

Similar hydrothermal experiments have been initiated for a phosphate-bonded castable refractory with tabular alumina aggregate. The only difference was the use of 5 ml. of water in the pressure chamber instead of 3 ml. Preliminary results at 110°C and 375°C have shown no reduction in flexural strength with hydrothermal treatment (see Figure 2). Analysis of the crystalline phases is still in progress.

In conjunction with task 1.A.b on Metal Wear and with the assistance of Dr. A. J. Liberatore of Morgantown Energy Research Center, exposure racks of metallic and ceramic specimens have been installed at two locations in the product-gas outlet line of the experimental gasifier at Morgantown. One panel gives three angles of impingement for which erosion rates can be examined; the other panel has two angles of impingement. The normal temperature-pressure conditions at the location of the racks are approximately 540°C (1,000°F) and 1 MPa (150 psi), respectively. The gas

flow rate is normally 120,000 standard cubic feet per hour and the major components of a typcial gas composition (by volume) are: 47.6% N_2, 18.2% CO, 13.6% H_2, 10.0% H_2O, 7.6% CO_2, 2.3% CH_4, 0.6% H_2S, 0.1% NH_3. Three castables are being exposed: H. W. Castolast G, Resco AA-22 and A. P. Green Lo-Abrade.

While removing the gas sample port to install the specimen panels, a small piece of the existing refractory lining in the outlet line was removed for a subsequent analysis. The location of the sample was adjacent to the outer steel shell where the normal temperature is 95°C (~ 200°F). The sample was very friable. Phases identified by x-ray diffraction in order of abundance are listed in Table 2. Also listed are the chemical analysis and phases (in order of abundance) of what is thought to be the pre-mixed lightweight insulating castable. It appears that the calcium-aluminate phases in the original castable have been carbonated.

Table 2. Analysis of lightweight insulating castable adjacent to the steel shell in the gas sample port of the gasifier at the Morgantown Energy Research Center. Phases in order of abundance.

Phases by x-ray diffraction		Chemical Analysis
from gasifier	dried basis*	dried basis
cristobalite (SiO_2)	anorthite (CAS_2)	38.4% Al_2O_3
calcite ($CaCO_3$)	gehlenite (C_2AS)	31.2% SiO_2
mullite (A_3S_2)	CA	22.4% CaO
α-quartz (SiO_2)	α-quartz (SiO_2)	4.8% Fe_2O_3
gibbsite (AH_3)	mullite (A_3S_2)	1.5% TiO_2
	CA_2	0.5% MgO
		0.2% Na_2O & K_2O
		0.8% loss on ignition

* Trace amount of as yet unidentified phase(s). Cristobalite, which is probably present, is masked by other phases.

Plans: Delivery and "check-out" of the hydrothermal research unit is expected towards the end of the next quarter. An apparatus is being designed which will allow removal of the interim hydrothermal vessel from the furnace at temperature. This procedure should accelerate the "cool-down" period for this vessel. Projected completion date is mid-April. Generic castable mixtures in the 90% + Al_2O_3 composition will be prepared and a series of hydrothermal experiments will commence using both the Morrey pressure vessels and the interim vessel. Both flexural

strength and fracture properties will be examined. Hydrothermal studies with subsequent room-temperature flexural strength and erosion studies will also continue on a phosphate-bonded castable. Additional specimens of the refractory lining from the gasifier at the Morgantown Energy Research Center are to be delivered for analysis. These specimens, which are a cross section of the lining, were obtained when a quench system was installed on the outlet gas line.

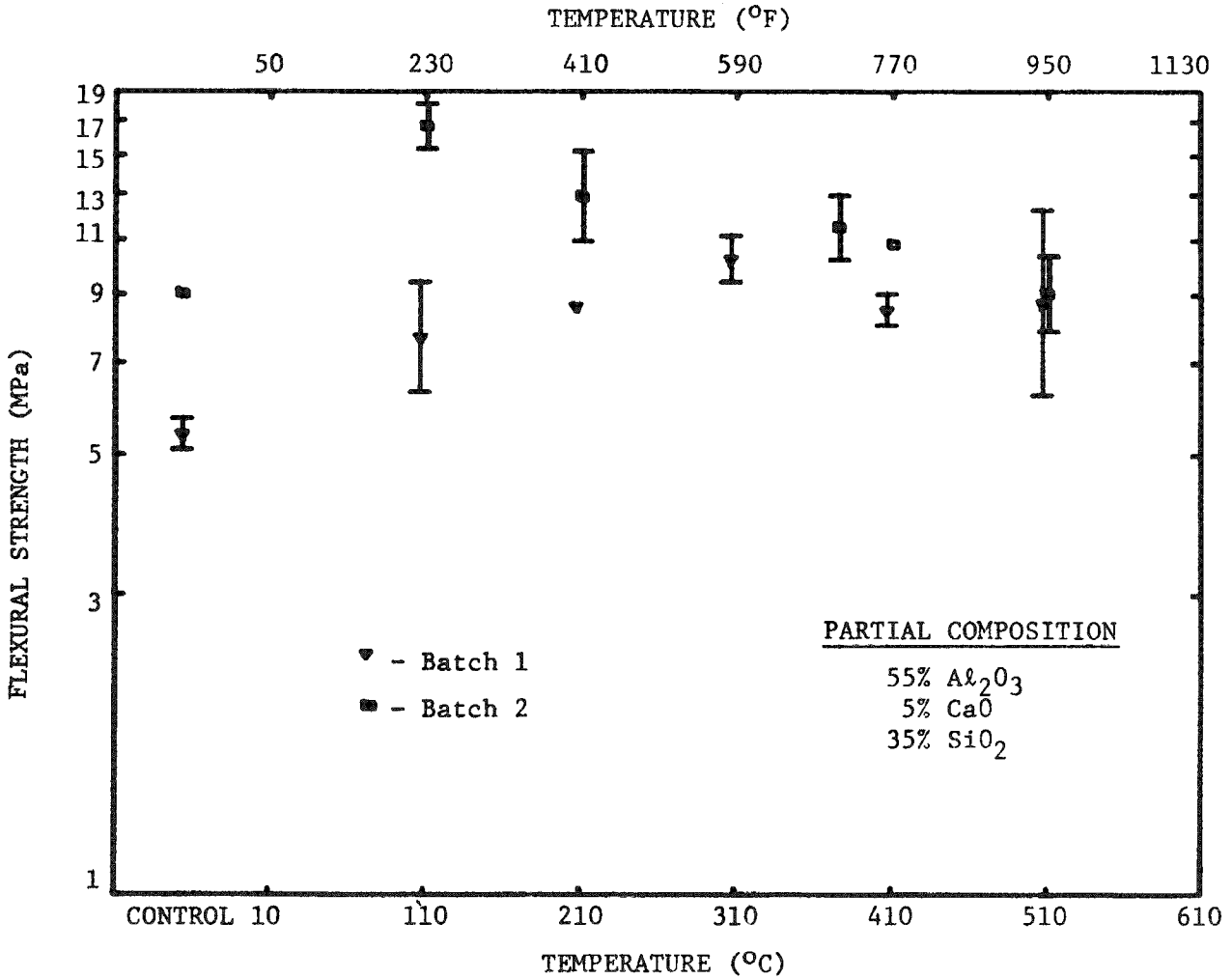

Figure 1. Effect of a 20 Hour Hydrothermal Treatment on the Flexural Strength of a Calcium-Aluminate-Bonded Castable Refractory with Calcined Flint Clay Aggregate. Specimens Prefired to 1010°C (1850°F).

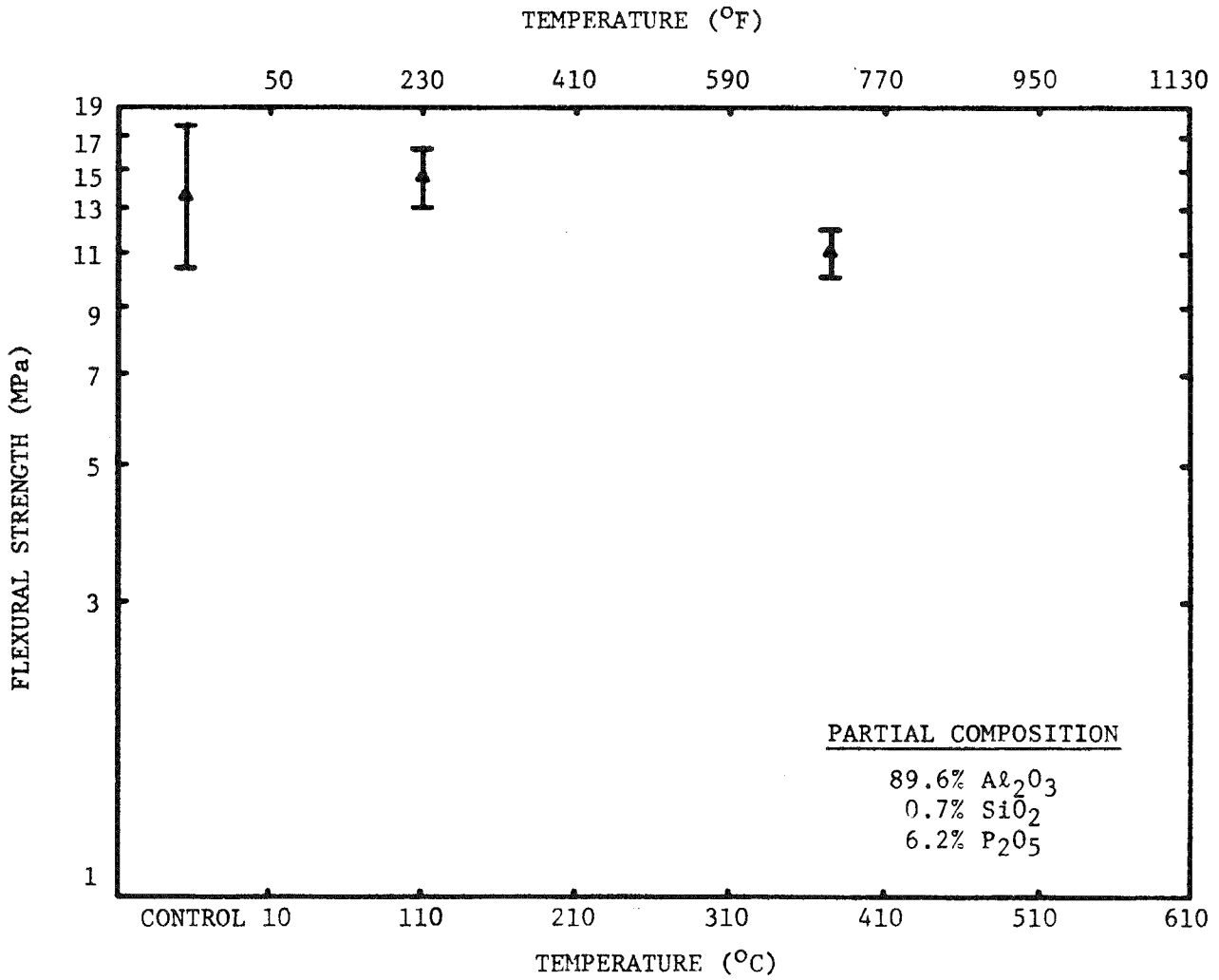

Figure 2. Effect of a 20 Hour Hydrothermal Treatment on the Flexural Strength of a Phosphate-Bonded Castable Refractory with Tabular Alumina Aggregate. Specimens Prefired to 1010°C (1850°F).

b) Erosive Wear (S. M. Wiederhorn, H. S. Siefert and D. E. Roberts, 313.05)

Progress: During the past quarter the effect of hydrothermal environments on the erosive wear of castable refractories was studied. These studies were part of a program to evaluate the influence of corrosive gases on refractories that are to be used to line the high temperature components of coal gasification plants. Because of its chemical reactivity with ceramic oxide refractories, high pressure steam is one of the gases that is expected to degrade the mechanical properties of these refractories. Earlier studies at NBS have shown that the strength of a high alumina castable refractory is severely degraded by high pressure steam. In this study it is shown that steam similarly effects the erosion resistance of this refractory.

Two types of refractories were studied. One was a high alumina castable refractory consisting of tabular alumina bonded with calcium aluminate. The other was made of calcined flint clay bonded with calcium aluminate. After casting the refractories into bars or plates and permitting them to "set" for 24 hours in an environment of 100 percent relative humidity, they were cut into one-half inch cubes which were then dried at 110°C for 24 hours. To obtain a refractory bond, the cubes were then heated in a furnace to 1000°C and held at this temperature for 5 hours. The chemical structure of the refractories was determined by X-ray diffraction analysis after this final heat treatment. The high alumina castable refractory consisted only of aluminum oxide (α-Al_2O_3) and calcium aluminate ($CaO.Al_2O_3$),while the calcined clay refractory consisted of cristobalite (SiO_2),mullite ($3Al_2O_3.2SiO_2$), two forms of calcium aluminate ($CaO.Al_2O_3$ and $CaO.2Al_2O_3$), an amorphous phase, and one unidentified crystalline phase. All erosion and hydrothermal studies were conducted on the castable refractories after they had been heated to 1000°C.

The hydrothermal treatments have been fully described in earlier reports on this project. Briefly, the cubes were sealed in a fixed volume (20 cc) Morey Bomb that contained approximately 3 cc of water. The bomb was then placed in a furnace, heated to the temperature of reaction and held for 20 hours. After cooling the bomb to room temperature and removing the specimens, they were permitted to dry in air for 24 hours to remove free water from the refractory. Although the refractories increased in strength when they were dried, removal of the water was necessary since evaporation of the water during the erosion studies would have interferred with the experiment.

Erosion studies were conducted at room temperature using an impingement angle of 90^{o}. Specimens were subjected to 100 gm of 100 mesh silicon carbide at velocities that ranged from 15 to 50 m/s. The erosion rate was determined from the total weight loss during each experiment. As in earlier studies erosion occurred mainly in the bonding matrix of the castable refractory, so that all results reported here relate to the erosion resistance of the bonding phase.

Results of the erosion studies are given in figures 1 and 2 which present the erosion rate as a function of the particle velocity and the temperature of the hydrothermal treatment. For the high purity aluminum oxide refractory (figure 1), the erosion rate increases abruptly when the temperature of the hydrothermal treatment is increased from 210°C to 375°C. By contrast, the erosion resistance of the flint clay refractory (figure 2) is relatively insensitive to the temperature of the hydrothermal treatment. The dependence of the erosion rate on the particle velocity is similar to that reported earlier. At each temperature, the erosion rate, R, can be expressed as a power function of the particle velocity, v, $R \propto v^{a}$, where the power exponent, a, has a value that ranged from 2.3 to 3.9 depending on the hydrothermal treatment. It is uncertain at the present time if this variation in the power exponent has any fundamental significance. Similar variations have been reported in the literature for other materials.

The dependence of erosion behavior on hydrothermal treatment is presented in figures 3 and 4 for a particle velocity of 29 m/s. The high purity aluminum oxide castable (figure 3) has an erosion rate of approximately 10^{-2} milligrams/gram of abrasive for hydrothermal temperatures of less than 210°C. The erosion rate increases by a factor of approximately 10 when the hydrothermal temperature is increased to 375°C. By contrast, the erosion rate of the calcined flint clay refractory (figure 4) is insensitive to the hydrothermal treatment over the entire range of temperature. The erosion data given in figures 3 and 4 can be compared with strength data (figures 5 and 6) obtained earlier in these studies. The abrupt decrease in strength of the high purity aluminum oxide castable (figure 5) occurs at the same temperature as the increase in erosion rate shown in figure 3. Similarly, the insensitivity of the erosion rate of the flint clay castable refractory (figure 4) to hydrothermal treatments is consistent with the insensitivity of the strength of this refractory (figure 6) to hydrothermal treatments. These results suggest that the erosion rate is controlled by the strength of the refractory, and that any change in strength will be accompanied by a similar change in erosion rate.

A tentative explanation for the change in the erosion resistance and the strength of the high purity aluminum oxide castable refractory has been obtained from X-ray diffraction analyses of the castable refractory. It has been observed that crystal phase changes occur as the castable refractory is subjected to various hydrothermal treatments. These phase changes have been discussed in an earlier report and will only be briefly reviewed here. Before exposing the high alumina refractory to hydrothermal treatments only aluminum oxide and calcium aluminate are present in the refractory. Hydrothermal treatments result in the formation of several hydrated calcium aluminate phases. The phase that is associated with the strength degradation is the boehmite that first forms in the refractory at temperatures ranging from 110°C to 210°C, and then decomposes at temperatures greater than 375°C. The boehmite apparently acts as a bonding phase in the matrix of the refractory and provides substantial strength to the matrix at temperatures up to 210°C. However, when this phase decomposes to form aluminum oxide, the bonding matrix loses its structural integrity and consequently a decrease in both the strength and the erosion resistance of the refractory is observed. By contrast the bonding phase of the calcined flint clay castable refractories contains other components (cristobalite and mullite) that maintain their integrity throughout the range of temperatures used for the hydrothermal treatment and as a consequence provide the strength for the matrix. The chemical stability of mullite and cristobalite account for the fact that strength degradation does not occur in the flint clay castable refractory.

This study demonstrates the importance of phase stability in the castable refractories that are being used as linings in coal gasification plants. Without phase stability serious degradation of the mechanical properties of the linings can significantly decrease the expected lifetime of these linings. In this study the importance of water as a reactive species was demonstrated. In the coal gas environment other reactions are likely to cause similar degradation of strength and erosion resistance. One objective of future studies in this program will be to identify chemical reactions and structural changes that reduce the mechanical integrity of refractories.

In addition to the study just described, the effect of erosion time on the erosion rate was investigated. The calcium aluminate bonded aluminum oxide refractory used in earlier studies was exposed to greater amounts of erosion particles than had been used previously. The objective of the study is to determine if the power function law observed for the initial stages of wear holds in later stages, and if the initial wear stage can be used to predict the wear of a ceramic refractory after long term exposure to erosion particles.

One-half inch cubes of refractory were exposed to 100 mesh silicon carbide particles at a velocity of 90 m/s at room temperature and 120 m/s at 1000°C. The results of these studies are shown in the figures 7 and 8 of this report. It was observed both at 25°C and 1000°C that an incubation period is apparently required before the refractory erodes at a steady state condition. At 25°C, the erosion rate for the first 25 grams of abrasive was nearly three times that obtained during steady state erosion. Above 100 grams total abrasive, the erosion rate was more or less independent of the amount of the abrasive used. By contrast, at 1000°C the incubation period required much less abrasive because higher velocities were used. At 1000°C, the erosion rate during the incubation period was considerably higher than that of the steady state condition. The decrease in erosion rate at 150 grams of abrasive is believed to be the result of holes being worn through the castable refractory so that the reading at 150 grams is incorrect.

Investigations of the effect of the exposure time on erosion have not yet been completed and as a consequence, it is still too early to draw firm conclusions on this effect. Studies of this type will be continued in the next quarter at the end of which time it is hoped to complete this aspect of the work.

Portions of the work discussed to date have been published in the Bulletin of the American Ceramic Society, 55, 185-189 (1976). In addition a paper entitled "Effect of Hydrothermal Environments on the Erosion of Castable Refractories" by S. M. Wiederhorn, E. R. Fuller and J. M. Bukowski will be presented at the annual winter meeting of the American Society for Mechanical Engineers to be held in New York, November 28 through December 3, 1976, in a seminar entitled "Wear by Erosion-Corosion". The work will be published in the proceedings of that conference.

Plans: During the next quarter work will be continued to evaluate the effect of exposure time on the wear rate. In addition other generic castable refractories will be investigated. To be included in these studies will be a phosphate bonded aluminum oxide refractory. The phosphate bonded refractory is expected to be more resistant to erosion than the other refractories studied. As in the earlier studies the wear rate will be measured as a function of impact velocity, erosion angle and temperature in order to evaluate the behavior of these refractories under a wide range of experimental conditions. Microstructural studies will be conducted to determine if the mechanism of wear of these refractories differs from that of the high aluminate calcium aluminate bonded refractory already investigated.

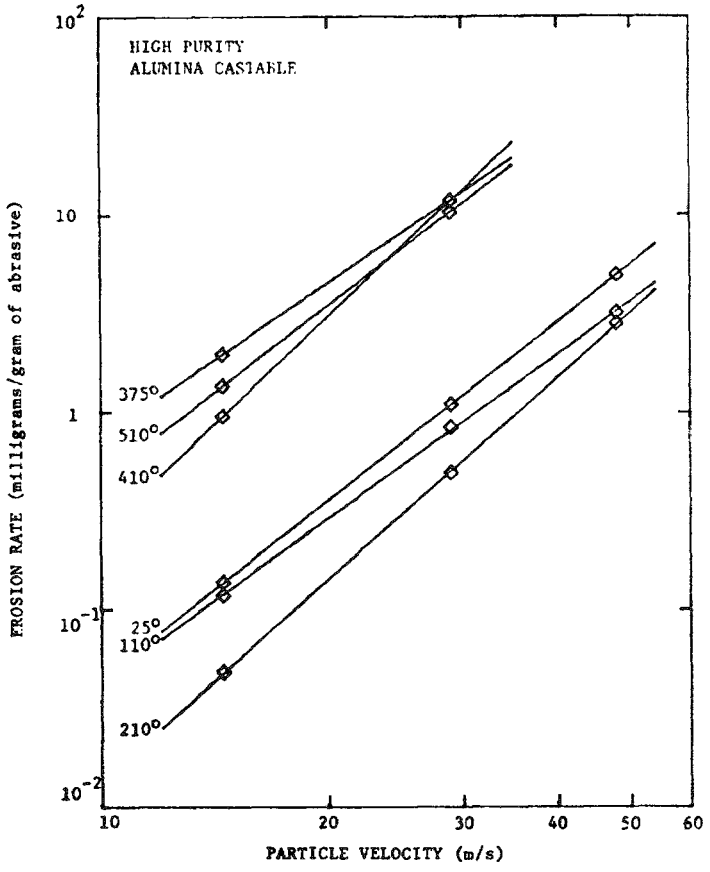

Figure 1. The erosion rate of a calcium aluminate bonded tabular alumina castable refractory as a function of the temperature of hydrothermal treatment and the particle velocity.

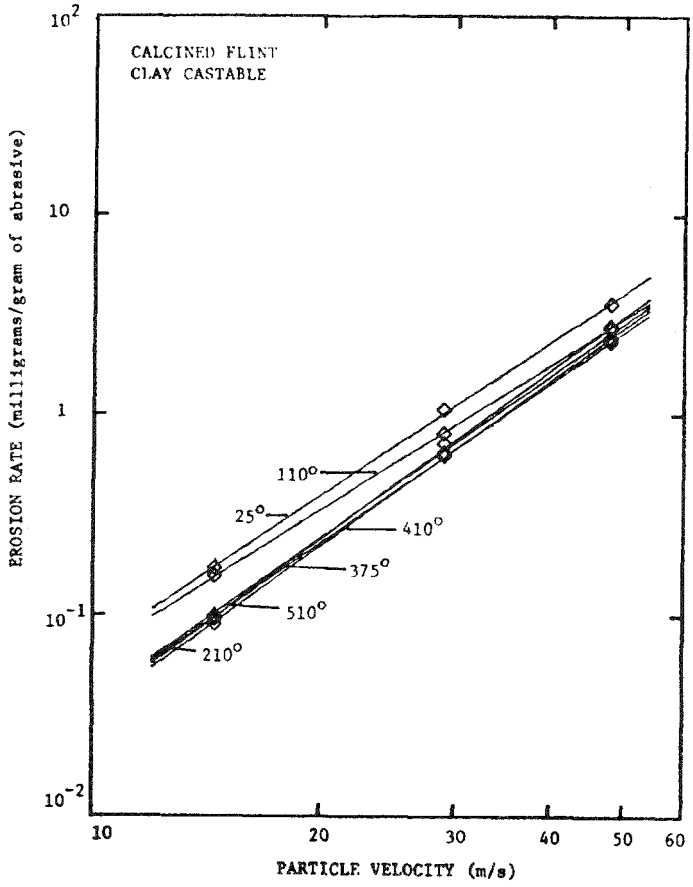

Figure 2. The erosion rate of a calcium aluminate bonded calcined flint clay refractory as a function of the temperature of hydrothermal treatment and the particle velocity.

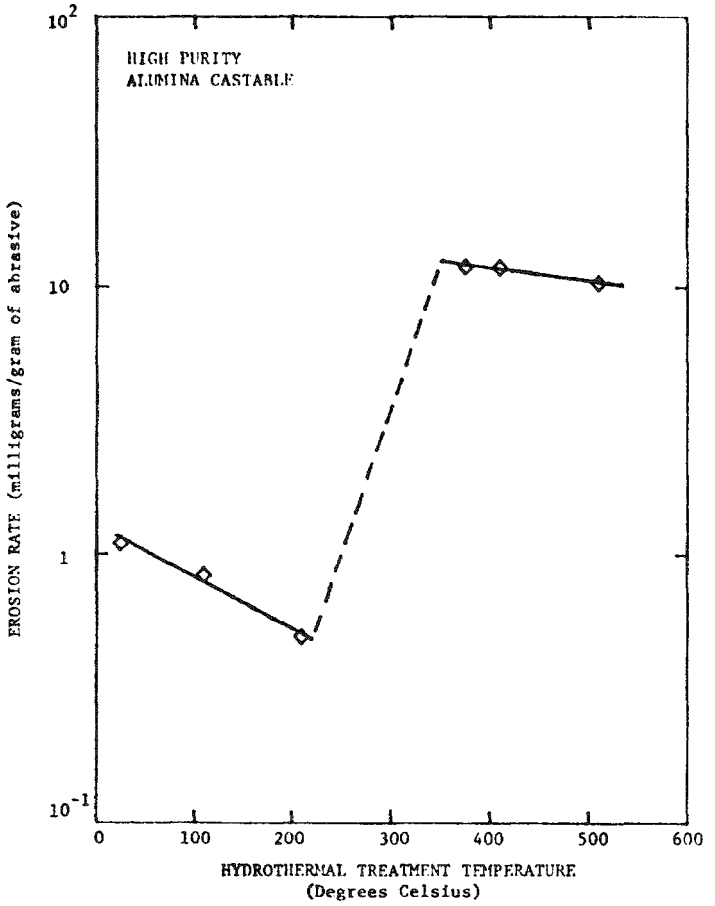

Figure 3. Erosion rate as a function of the temperature of hydrothermal treatment. Calcium aluminate bonded tabular alumina refractory eroded by 100 mesh SiC particles at a velocity of 29 m/s.

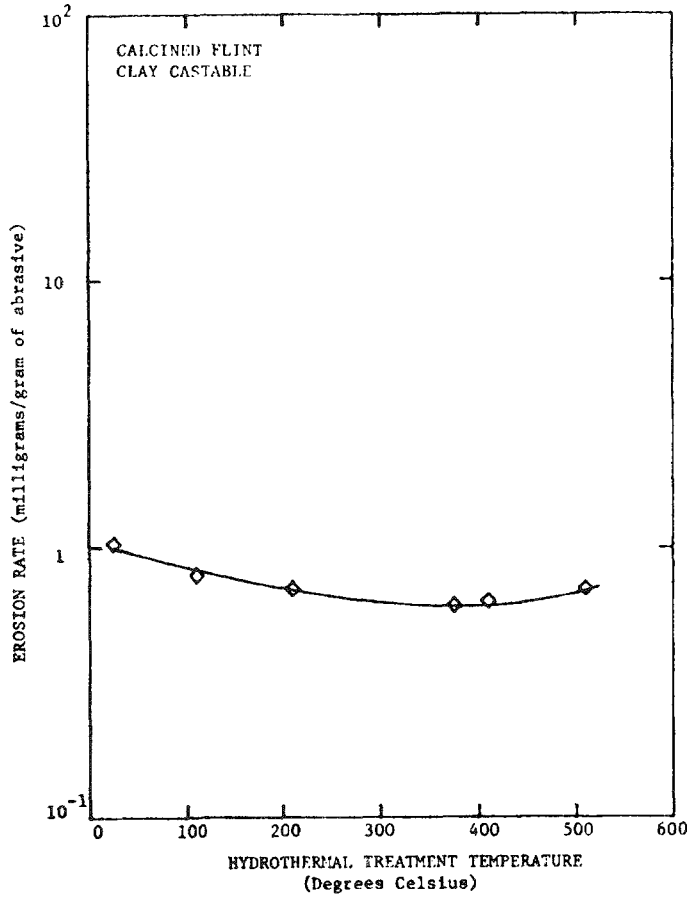

Figure 4. Erosion rate as a function of the temperature of hydrothermal treatment. Calcium aluminate bonded calcined flint clay refractory eroded by 100 mesh SiC particles at a velocity of 29 m/s.

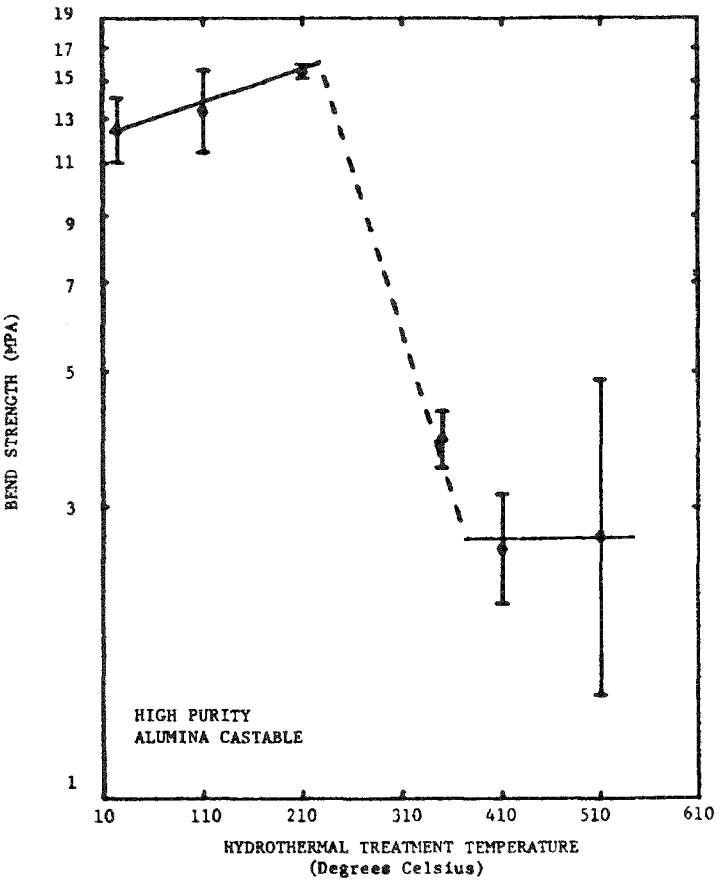

Figure 5. Strength of a calcium aluminate bonded tabular alumina castable refractory as a function of the temperature of hydrothermal treatment.

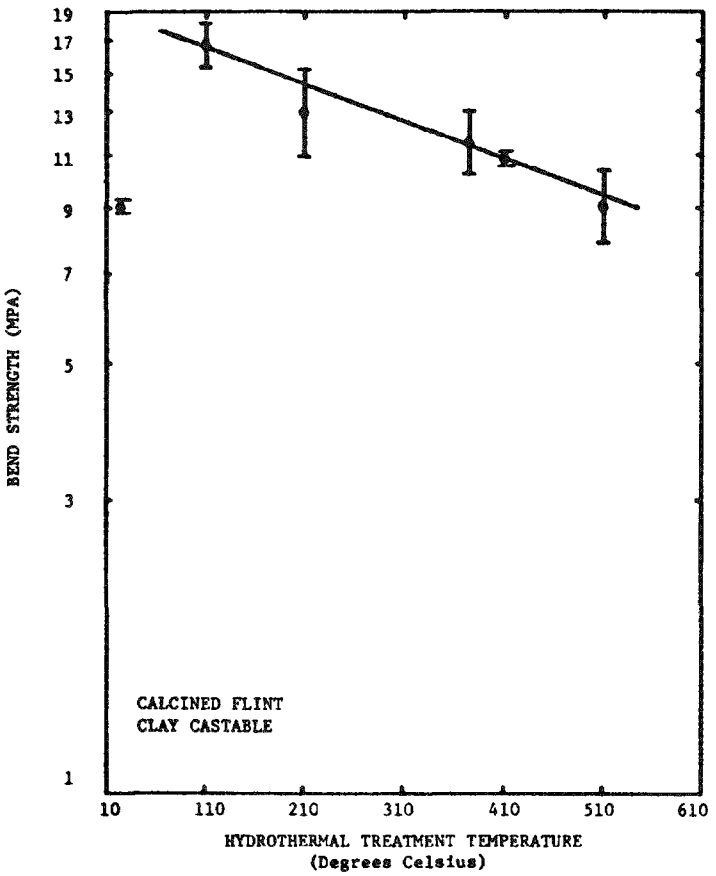

Figure 6. Strength of a calcium aluminate bonded calcined flint clay castable refractory as a function of the temperature of hydrothermal treatment.

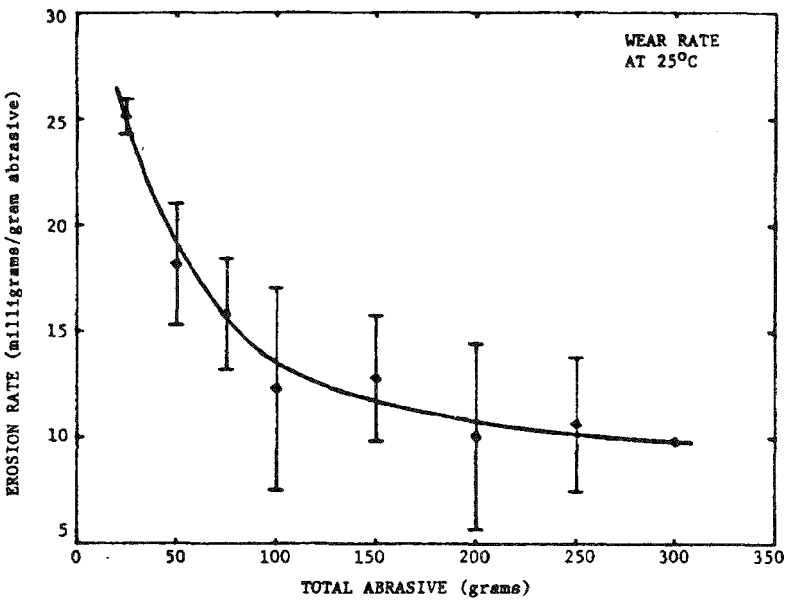

Figure 7. Erosion rate of a calcium aluminate bonded tabular alumina castable refractory as a function of the total weight of abrasive. Tests conducted at 25°C using 100 mesh SiC particles at a velocity of approximately 60 m/s.

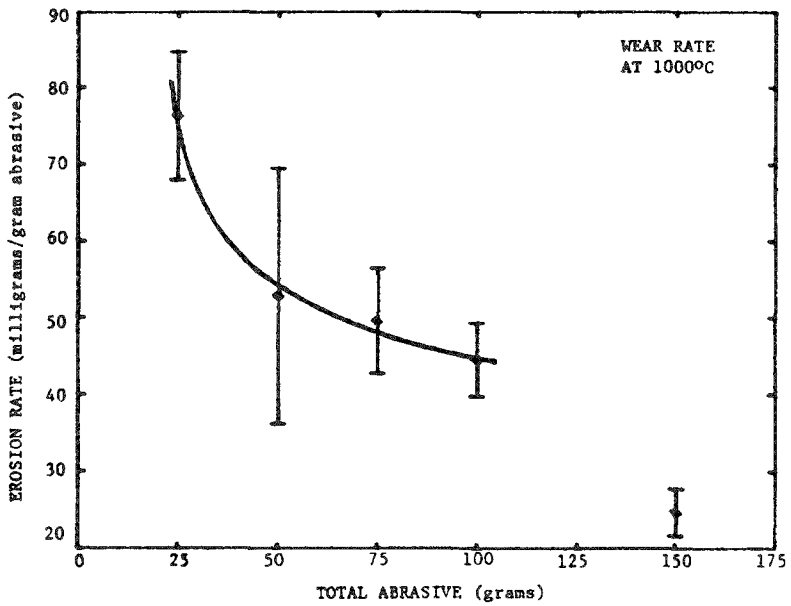

Figure 8. Erosion rate of a calcium aluminate bonded tabular alumina castable refractory as a function of the total weight of abrasive. Tests conducted at 1000°C using 100 mesh SiC particles at a velocity of approximately 90 m/s.

2. Chemical Degradation of Ceramics (W. S. Brower, J. L. Waring and C. A. Harding, 313.03)

a. Gas Phase Reactions

Progress: The work in the system $CaO \cdot Al_2O_3 \cdot H_2O$ at 1000 psi (steam) is essentially complete. A constitution diagram (Figure 1) has been constructed from the data given in Table 1. From Figure 1 it can be seen that the first hydrate formed $3CaO \cdot Al_2O_3 \cdot 6H_2O$ is unstable and dissociates above room temperature to form $Ca(OH)_2$ and $4CaO \cdot 3Al_2O_3 \cdot 3H_2O$. Preformed $3CaO \cdot Al_2O_3$ was found to have a minimum dissociation temperature in excess of 1000°C at 1000 psi stem. The 1000°C/1000 psi data was obtained with the TZM apparatus which was made operational this reporting period. The maximum and minimum dissociation temperature for the $12CaO \cdot 7Al_2O_3$ hydrogarnet have not been established. However the minimum temperature of formation is probably in excess of 400°C and the compound should be stable to the reported melting point of about 1392°C. The hydrate $4CaO \cdot 3Al_2O_3 \cdot 3H_2O$ has a minimum temperature of stability below 200°C and a maximum temperature of stability below 600°C in 1000 psi steam. $CaO \cdot Al_2O_3$ and $CaO \cdot 2Al_2O_3$ were found to exist at temperatures in excess of 1000°C and to hydrate below about 400°C. The compounds $CaO \cdot Al_2O_3$, $CaO \cdot 2Al_2O_3$ and $CaO \cdot 6Al_2O_3$ experimentally appear to have the same minimum temperature of stability since at these relatively low temperatures the reactions proceed very slowly and it has not been posible to delineate these boundaries, therefore the region of uncertainty is shaded on the diagram. At a temperature below about 400°C-450°C these phases dissociate into boehmite and $4CaO \cdot 3Al_2O_3 \cdot 3H_2O$. The phase transition between boehmite and Al_2O_3 in the pressure range of 1000 psi is currently under investigation.

In conclusion at 1000 psi of steam a refractory cement consisting of a mixture of $CaO \cdot 2Al_2O_3$, $CaO \cdot Al_2O_3$ and Al_2O_3 grog might be expected to react slowly at about 450°C. The $3CaO \cdot Al_2O_3 \cdot 6H_2O$ originally formed in the cement will transform rapidly to form 4CaO Al 0 3H 0, which will then slowly react to form first $12CaO \cdot 7Al_2O_3$ plus $CaO \cdot Al_2O_3$ and then eventually $CaO \cdot 6Al_2O_3$ plus Al_2O_3.

Some preliminary work has been completed in the system $CaO \cdot Al_2O_3$ H_2O with high pressure CO_2 (860 psi) the data are given in Table 2. At 700°C (860 psi) $3CaO \cdot Al_2O_3$ decomposes to $12CaO \cdot 7Al_2O_3$ and $CaCO_3$. When $3CaO \cdot Al_2O_3 \cdot 6H_2O$ was heated to 800°C (860 psi) $CaO \cdot 2Al_2O_3$ was heated to 800°C (860 psi) $CaO \cdot 2Al_2O_3$ and $CaCO_3$ were formed. In addition a new phase (major x-ray line 3.705A) was found to be present.

Plans: The boehmite - Al_2O_3 phase transition will be investigated in the pressure range of 1000 psi as the appearance of boehmite seems to be related to strength of alumina castables (Fuller this report). Attempts will be made to prepare the new phase formed on the decomposition of the $3Al_2O_3 \cdot Al_2O_3 \cdot 6H_2O$ in a more crystalline form so that it can be identified and its stability range determined.

b. Slag-Refractory Interactions

Progress: Additional slag samples have been prepared in the form of right cylinders for solid state diffusion studies with candidate refractory materials. The high pressure (300 psi) crystal growth apparatus is in the process of being modified for slag viscosity measurements as a function of pressure using $CO-CO_2$ mixtures. The preliminary design of apparatus for high temperature viscosity measurements in a pressurized steam atmosphere have been completed. The essential part of the heating apparatus (1-4 volt 10KVA transformer) has been obtained.

Plans: The reaction of slag with various generic refractories will be studied by measuring penetration depth of the slag components at temperatures up through the softening point of the slag.

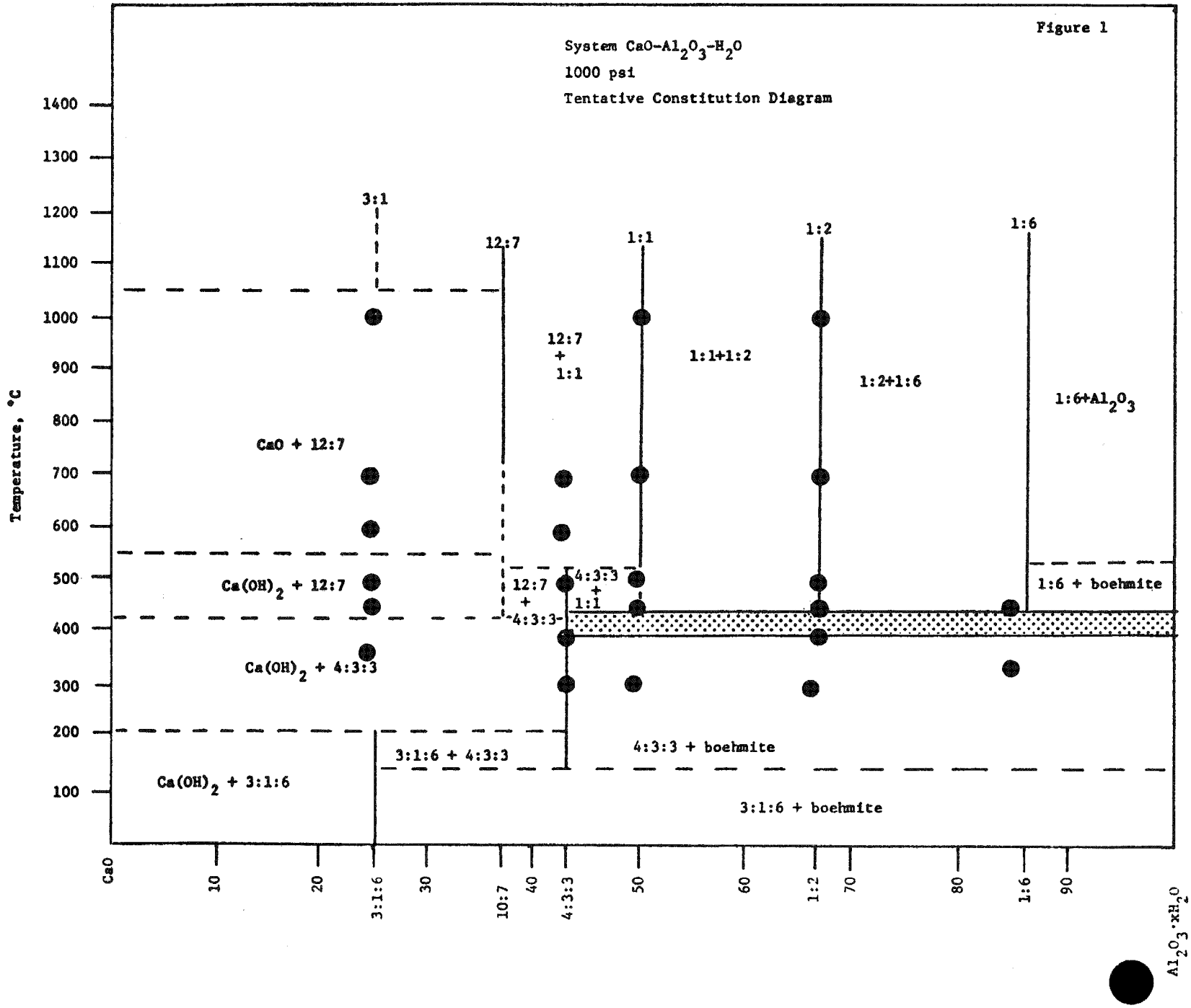
Figure 1
System CaO-Al2O3-H2O
1000 psi
Tentative Constitution Diagram
Temperature, °C
1400
1300
1200
1100
1000
900
800
700
600
500
400
300
200
100
3:1
12:7
1:1
1:2
1:6
12:7 + 1:1
1:1+1:2
1:2+1:6
1:6+Al2O3
CaO + 12:7
Ca(OH)2 + 12:7
Ca(OH)2 + 4:3:3
12:7 + 4:3:3
4:3:3 + 1:1
1:6 + boehmite
4:3:3 + boehmite
3:1:6 + 4:3:3
Ca(OH)2 + 3:1:6
3:1:6 + boehmite
CaO
10
20
3:1:6
30
10:7
40
4:3:3
50
60
1:2
70
80
1:6
90
Al2O3·xH2O

Table I. Experimental Data for the System $CaO-Al_2O_3-H_2O$ at 1000 psi Steam Pressure.

Starting Material[1/]	Temp. °C	Pressure psi	Time hrs	X-ray Diffraction Analysis	Conclusions
3:1:6	350	1000	720	4:3:3 + $Ca(OH)_2$ + hydrate	3:1:6 → 4:3:3 + hydrate
3:1:6	450	1000	720	4:3:3 + $Ca(OH)_2$ + 3:1:6 + hydrate	3:1:6 → 4:3:3 + hydrate
3:1	350	1000	720	3:1 + $Ca(OH)_2$ + 12:7	3:1 → 12:7 + $Ca(OH)_2$
3:1	450	1000	720	3:1 + $Ca(OH)_2$ + 12:7	3:1 → 12:7 + $Ca(OH)_2$
3:1	500	1000	168	3:1 + 12:7 + $Ca(OH)_2$	3:1 → 12:7 + $Ca(OH)_2$
3:1	600	1000	168	12:7 + 3:1 + CaO	3:1 → 12:7 + CaO
3:1	700	1000	168	3:1 + 12:7 + CaO	3:1 → 12:7 + CaO
3:1	1000	945	120	12:7 + CaO	3:1 → 12:7 + CaO
4:3:3	350	1000	720	4:3:3 + boehmite	$Ca(OH)_2$ + amorphous Al_2O_3 + 4:3:3 → 4:3:3 + boehmite
4:3:3	400	1000	86	4:3:3 + $Ca(OH)_2$	4:3:3 + amorphous $Ca(OH)_2$ + amorphous Al_2O_3 → 4:3:3 + $Ca(OH)_2$
4:3:3	450	1000	720	4:3:3	4:3:3 + amorphous $Ca(OH)_2$ + amorphous Al_2O_3 → 4:3:3
4:3:3	500	1000	86	4:3:3 + $Ca(OH)_2$	4:3:3 + amorphous $Ca(OH)_2$ + amorphous Al_2O_3 → 4:3:3 + cryst $Ca(OH)_2$
4:3:3	500	1000	168	4:3:3	4:3:3 + amorphous Al_2O_3 + amorphous $Ca(OH)_2$ → 4:3:3 + $Ca(OH)_2$
4:3:3	600	1000	168	4:3:3 + 12:7 + CaO	4:3:3 + 12:7 + CaO
4:3:3	700	1000	168	(leaked) 12:7 + 1:1	-----
1:1	300	1000	168	4:3:3 + 1:1 + boehmite	1:1 → boehmite + 4:3:3
1:1	400	1000	240	1:1	1:1
1:1	450	1000	240	1:1 + 4:3:3	1:1 → 4:3:3
1:1	500	1000	264	1:1	1:1 → 1:1
1:1	700	1000	168	1:1 + 1:2	1:1 → 1:1
1:1	1000	945	120	1:1	1:1 → 1:1
1:2	300	1000	168	1:2 + 4:3:3 + boehmite	1:2 → boehmite + 4:3:3 + boehmite
1:2	400	1000	264	1:2 + boehmite + 4:3:3	1:2 → boehmite + 4:3:3
1:2	450	1000	240	1:2	1:2 → 1:2
1:2	500	1000	264	1:2	1:2 → 1:2
1:2	700	1000	168	1:2	1:2 → 1:2
1:2	1000	945	120	1:1	1:1 → 1:2
1:6	350	1000	945	1:6 + 4:3:3 + Al_2O_3	1:6 → 4:3:3 + boehmite + Al_2O_3
1:6	450	1000	945	1:6 + Al_2O_3	1:6 → 1:6 + Al_2O_3

[1/] 3:1:6 = $3CaO:Al_2O_3:6H_2O$
1:2 = $CaO:2Al_2O_3$
3:1 = $3CaO:Al_2O_3$
4:3:3 = $4CaO:3Al_2O_3:3H_2O$
12:7 = $12CaO:7Al_2O_3$
1:1 = $CaO:Al_2O_3$
1:6 = $CaO:6Al_2O_3$

Table II. Experimental Data for the System $CaO-Al_2O_3-H_2O$ at 860 psi CO_2.

Starting Material[1/]	Temp. °C	Pressure psi	Time hrs	X-ray Diffraction Analysis	Conclusions
3:1:6	800	860	168	1:2 + $CaCO_3$ + unknown major line 24.00° $2\theta^3$	3:1:6 → 1:2 + $CaCO_3$ + unknown
3:1	600	860	72	3:1 + tr 12:7 (?)	3:1 → 3:1
3:1	700	860	72	3:1 + 12:7 + $CaCO_3$	3:1 → 12:7 + $CaCO_3$
4:3:3	700	860	168	1:1 + $CaCO_3$ + unknown	4:3:3 → 1:1 + $CaCO_3$ + unknown
4:3:3	800	860	168	$CaCO_3$ + unknown + 1:2	4:3:3 → 1:2 + $CaCO_3$ + unknown + 1:1
1:1	600	860	72	1:1	1:1 → 1:1
1:1	700	860	144	1:1 + tr 1:2	1:1 → 1:2
1:1	800	860	144	1:1	1:1 → 1:1
1:2	700	860	144	1:2	1:2 → 1:2
1:6	700	860	144	1:6	1:6 → 1:6

[1/] 3:1:6 = $3CaO:Al_2O_3:6H_2O$
1:2 = $CaO:2Al_2O_3$
3:1 = $3CaO:Al_2O_3$
4:3:3 = $4CaO:3Al_2O_3:3H_2O$
12:7 = $12CaO:7Al_2O_3$
1:1 = $CaO:Al_2O_3$
1:6 = $CaO:6Al_2O_3$

3. Consultation and Proposal Review

Progress: During the reporting period nine proposals were evaluated for ERDA/FE.

Plans: Consultation and proposal reviews will continue as requested by ERDA.

4. Failure Analysis (J. H. Smith, 312.01)

A. Failure Avoidance Program

Progress: Information about pilot plant operating incidents and component failure experiences has been obtained from the CO_2 acceptor process, Hygas, Synthane, Project Lignite, Solvent Refined Coal, and U.S.S. Clean Coke pilot plants. This information has been cataloged for future reference and access. The information has been classified according to source, pilot plant, materials type, failure category, and type of component. Detailed abstracting and evaluation of the information received is done on a continuing basis. The abstracts are cross indexed by the categories listed above for easy access. This procedure has made it possible to identify the most common and frequently occurring materials problems and failure categories. A summary of the frequency of the most common types of failures experienced to date is shown in Table 1.

In addition to information received from the operating pilot plants, the Failure Avoidance Program will include relevant information on the properties and performance of materials for use in coal conversion processing equipment. To facilitate the collection of this type of information, the annual review meeting of the Metals Property Council Committee on Materials for Coal Gasification Processes was attended and the progress reports issued to date were obtained. This information will be evaluated and included in the Failure Avoidance Program data base.

To implement the information dissemination part of the Failure Avoidance Program, a presentation was made at the February 26th meeting of the ERDA program managers. This meeting was attended by staff members from the Fossil Energy Administration Office of ERDA, the program managers responsible for each of the coal conversion pilot plants, and representatives from the failure analysis groups at Argonne, Oak Ridge, and Sandia-Livermore laboratories. The presentation outlined the objectives of the Failure Avoidance Program, showed the expected information flow diagram (Figure 1) and gave a summary of the most frequent types of failures experienced in the pilot plants (Table 1).

The establishment of the Failure Avoidance Information Data Center has been initiated. This involves filing the abstracts of all items of information on pilot plant operating incidents according to categories described above. At present, this is done by copying the abstracts on cards and accessing the information manually. As the amount of information increases, accessing the information manually will become increasingly

inefficient and expensive. Therefore, a computer assisted information storage and retrieval system known as a Data Base Management System will be necessary for handling the failure avoidance information. The NBS Computer Systems and Software Division personnel have given assistance in choosing a suitable system for this purpose and have chosen a Computer Corporation of America, system 204 for this use.

Plans: The information gathering and evaluation of the Failure Avoidance Program will continue and will include completion of the abstracting, evaluation, and indexing of the backlog of information received to date. Follow-up to obtain additional information on the operating incidents will be initiated. It is planned to visit each of the currently operating pilot plants to review in detail the failure incidents experience.

The information dissemination part of this program will include a presentation at the Mechanical Failures Prevention Group meeting on "Prevention of Failures in Coal Conversion Systems" in Columbus, Ohio on April 21 to 23, 1976. This presentation will include an outline of the Failure Avoidance Program and a summary of results obtained to date.

The work planned for the Failure Avoidance Information Data Center part of this program will include the necessary training to implement the use of the CCA system 204 data base management system for storing and accessing the information presently available on the manually accessible information system will be transferred to the system 204. The Fossil Energy Administration Office senior staff are in the process of implementing a reliability program for all pilot and demonstration plants. They plan to use the Government and Industry Data Exchange Program (GIDEP) to store and access information on the reliability of materials and components. Liaison will be closely maintained with this reliability program so that the information contained in the Failure Avoidance Information Data Center will be available through the GIDEP system.

B. Diagnostic Failure Analysis

Progress: Sections of thermocouple protection tubes and recycle heater coils that had failed in service at the CO_2 acceptor process pilot plant have been examined and analysed. Chemical analysis showed that the thermocouple protection tubes were 310 stainless steel. Metallographic examination indicated that high temperature sulfidation was the cause of failure. One recycle heater coil was Inconel 702 and one was Incoloy 800. Metallographic examination suggested that both heater coils were subjected to severe high temperature sulfidation. Electron microprobe analysis is being conducted on both the thermocouple protection tubes and the heater coils to identify the corrosion products and establish more exactly the mechanism of degradation.

Plans: The diagnostic failure analysis of the failed thermocouple protection tubes and the recycle heater coils will be completed and a brief report will be issued.

Diagnostic failure analysis of the fialed components from the Project Lignite process development unit will be initiated in cooperation with Oak Ridge National Laboratory.

Failure Avoidance:
Information Flow Diagram

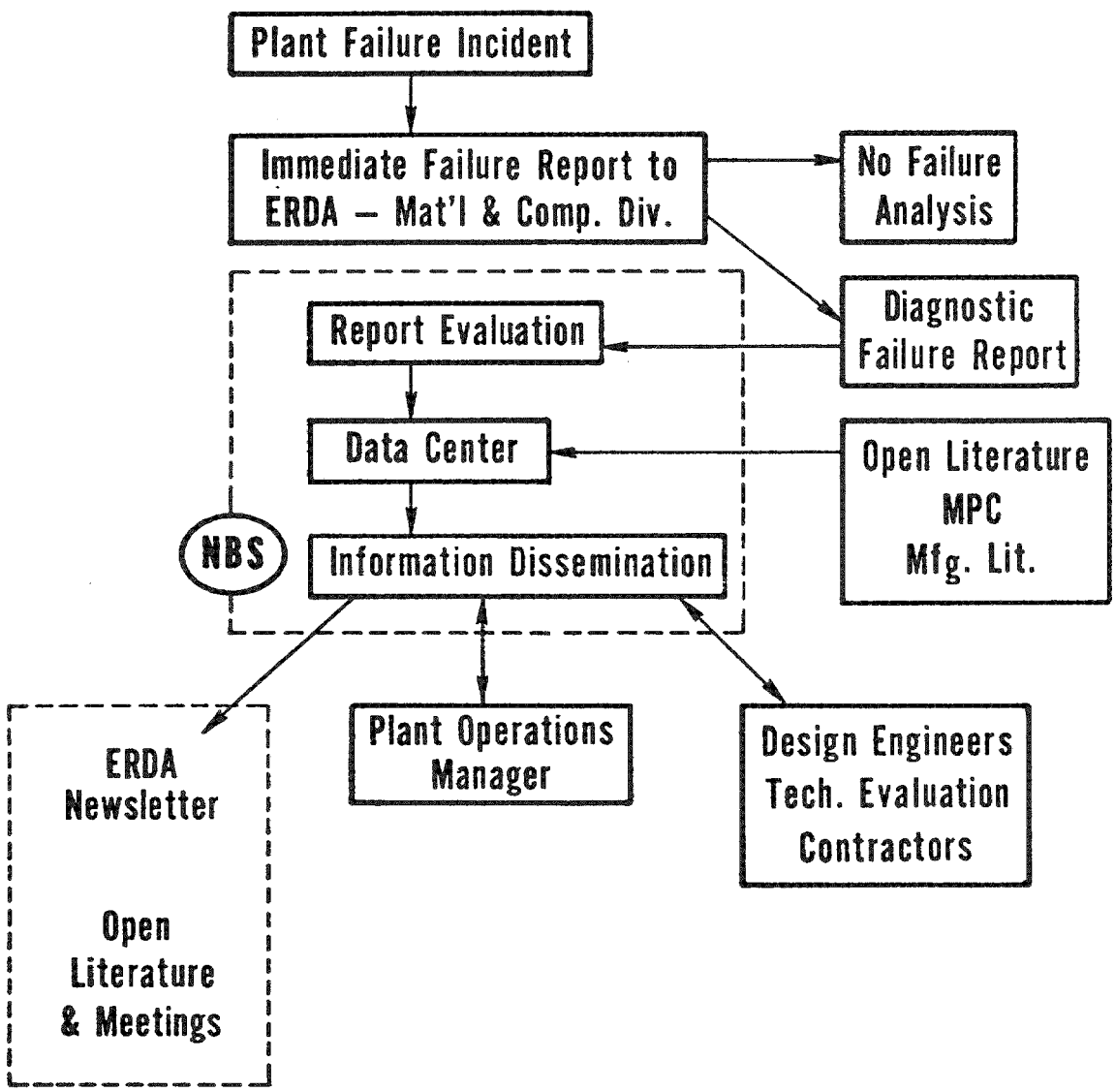

Figure 1.

Table I. Summary of Failure Incidents in Coal Conversion Systems

Cause of Incident	No. of Incidents	Coal Conversion Process					
		A	B	C	D	E	F
Undetermined	12	2	4	4	2		
Sulfidation	11	10	1				
Erosion	10	3		5	1		1
Corrosion	8	2	3	1	1		1
Design Defect	7	1	2	4			
SCC - Chloride	5	3	1			1	
Fabrication Defect	4	1	3				
Quality Control					1		
Refractory		1					

LIST OF PUBLICATIONS AND TALKS

Publications:

1. "A Technique to Investigate High Temperature Erosion of Refractories," S. M. Wiederhorn and D. E. Roberts, Bul. Am. Ceramic Soc. 55, 185-189 (1976)

2. "Constant Strain-Rate Stress Corrosion Testing at Elevated Temperatures," G. M. Ugiansky and C. E. Johnson, MFPG (Mechanical Failures Prevention Group) Symposium on Prevention of Failures in Coal Conversion Systems, April 21-23, 1976, Battelle Columbus Labs, Columbus, Ohio

3. "Measurement of Solid Particle Velocity in Erosive Wear," A. W. Ruff and L. K. Ives, National Bureau of Standards, Washington, D. C. 20234, May 5, 1975, Wear, 35 (1975) 195-199

4. "Particle Erosion Measurements on Metals," J. P. Young and A. W. Ruff National Bureau of Standards, Washington, D. C. 20234 (submitted to Trans. ASME)

5. "Erosion of Stainless Steel and Nickel Base Alloys at 1000°C," L, K. Ives, National Bureau of Standards, Washington, D. C. 20234 (to be submitted to Trans. ASME)

6. "Particle Erosion Measurements on Metals at Elevated Temperatures," L. K. Ives, J. P. Young, and A. W. Ruff, National Bureau of Standards, Washington, D. C. 20234 (to be submitted to Mech. Failure Prevention Symposium April 1976)

7. "Erosion Measurements on Metals at Elevated Temperatures," L. K. Ives, J. P. Young, and A. W. Ruff, National Bureau of Standards, Washington, D. C. 20234 (to be submitted at the Second International Conference on Mechanical Behavior of Materials)

Talks:

1. "Effect of Elevated Pressure Steam on the Strength of Refractory Castables," E. R. Fuller and C. R. Robbins, Am. Ceramic Soc., Refractories Div. Fall Mtg. Oct. 2-4, Beford, Pa.

2. "Constant Strain-Rate Stress Corrosion Testing for Coal Gasification Systems," G. M. Ugiansky and C. E. Johnson, Workshop on Materials Technology for Coal Gasification, Sept. 11-12, 1975, National Bureau of Standards, Gaithersburg, Md.

3. "Constant Strain-Rate Stress Corrosion Testing," G. M. Ugiansky and C. E. Johnson, ASM-AIME Annual Mtg., 1975 Materials Science Seminar, Nov. 13, 1975, Cincinnati, Ohio

Talks (continued)

4. "Constant Strain-Rate Stress Corrosion Testing for Coal Gasification Systems," G. M. Ugiansky and C. E. Johnson, CORROSION/76, NACE Annual Mtg., Corrosion Research Conference, March 22-24, 1976, Houston, Texas.

5. "Constant Strain-Rate Stress Corrosion Testing at Elevated Temperatures," G. M. Ugiansky and C. E. Johnson, MFPG Symposium on Prevention of Failures in Coal Conversion Systems, April 21-23, 1976, Battelle Columbus Labs, Columbus, Ohio

6. "Erosion Measurements on Metals at Elevated Temperatures," A. W. Ruff, J. P, Young and L. K. Ives, ERDA/FE Meeting at NBS on Sept. 11-12, 1975.

7. "Erosion/Corrosion Measurements on Metals," A. W. Ruff, L. K. Ives, and J. P. Young, ASM Symposium on Materials Behavior in Coal Gasification Environments, Nov. 10, 1975, Cleveland, Ohio

8. "High Temperature Erosion in Oxidizing and Reducing Atmospheres," A. W. Ruff, J. P. Young, and L. K. Ives, abstract for ASM Conference on Materials for Coal Confersion Systems Design, April 26, 1976, Pittsburgh, Pa.

9. "Particle Erosion Measurements on Metals," J. P. Young and A. W. Ruff, Am. Soc. Mech. Engin., New York, December 1, 1976

10. "Erosion of Stainless Steel and Nickel Base Alloys at 1000°C," L. K. Ives, Am. Soc. Mech. Engin., New York, December 1, 1976

11. "Particle Erosion Measurements on Metals at Elevated Temperatures," L. K. Ives, J. P. Young, and A. W. Ruff, MFPG, Columbus, Ohio, April 21, 1976

12. "Erosion Measurements on Metals at Elevated Temperatures," L. K. Ives, J. P. Young, and A. W. Ruff, Second International Conference on Mechanical Behavior of Materials, Boston, Mass., August 16, 1976